

2014

Case Study of Accidental Confined Natural Gas Detonations and Associated Damage

Omar M. Alawad
Lehigh University

Follow this and additional works at: <http://preserve.lehigh.edu/etd>

 Part of the [Civil and Environmental Engineering Commons](#)

Recommended Citation

Alawad, Omar M., "Case Study of Accidental Confined Natural Gas Detonations and Associated Damage" (2014). *Theses and Dissertations*. Paper 1408.

This Thesis is brought to you for free and open access by Lehigh Preserve. It has been accepted for inclusion in Theses and Dissertations by an authorized administrator of Lehigh Preserve. For more information, please contact preserve@lehigh.edu.

Case Study of Accidental Confined Natural Gas Detonations and Associated
Damage

by

Omar Mohammed Alawad

A Thesis

Presented to the Graduate and Research Committee
of Lehigh University
in Candidacy for the Degree of
Master of Science

In

Structural Engineering

Lehigh University

September 2014

This thesis is accepted and approved in partial fulfillment of the requirements for the Master of Science.

Date

Clay J. Naito
Thesis Advisor

Panos Diplas
Chairperson of Department

Acknowledgments

First, I would like to thank my great parents who support me with throughout my life and for their encouragement and love. Also, special thanks to my lovely wife for her patient and continuous support.

I would like also to thank my advisor Prof. Clay J. Naito. I truly appreciate all of the support, advice, and guidance you have provided me throughout my master's degree in Lehigh University. I'm also grateful for the support provided by Christina Cercone.

Finally I would like to thank Qassim University for supporting me financially to pursue my master's degree in Lehigh University.

Table of Contents

Acknowledgments	v
List of Figures	ix
List of Tables	xiii
1. Abstract	1
2. Introduction.....	2
3. Natural Gas Accidents.....	4
4. Possible Scenarios of a Fuel Gas Release	8
5. Vapor cloud explosion (VCE)	10
5.1. Demand Estimation Procedures for VCE	12
5.1.1. TNT equivalent method.....	12
5.1.2. TNO multi-energy method.....	13
5.1.3. The Baker-Strehlow-Tang (BST) method.....	15
6. Estimated scenarios for both accidents (Allentown and Harlem)	20
7. Allentown case study.....	23
7.1. Center of Blast	25
7.2. The broken glass window	26
7.2.1. Dimensions of the broken glass window	26
7.2.2. Failure load of a glass window.....	28

7.3. Reflected pressure (<i>Pra</i>) and incident pressure (<i>Pso</i>):	29
7.4. Pressure prediction	31
7.4.1. Predicting pressure by the TNO method	31
7.4.2. Predicting pressure by BST method	33
7.4.3. Modified Bernoulli equation (MBE)	37
7.5. Associated damage and injuries for Allentown's incident	39
7.5.1. Associated damage and injuries within 20 ft from cloud center.....	39
7.5.2. Associated damage between 30 to 185 ft	41
7.5.3. Associated damage at 450 ft from cloud center	43
8. New York case study.....	45
8.1. Center of blast.....	45
8.2. Selection of the broken glass window	46
8.3. Pressure prediction	49
8.3.1. TNO and BST method.....	49
8.4. Associated damages and injuries for New York's incident	50
8.4.1. Associated damages and injuries within 30 ft from cloud center	50
8.4.2. Associated damage between 30 to 250 ft	51
8.4.3. Associated damage between 250 to 450 ft	52
8.5. Nonfactored and reflected load on glass window	55

8.6. Modified Bernoulli equation (MBE) (Harlem's accident)	57
9. Doubling explosion energy for both accidents (Allentown and Harlem)	58
10. Conclusion	61
11. References	62
Appendix A: Overpressure prediction for Allentown's accident	67
Appendix B: Reflected pressure coefficient	68
Appendix C: Incident pressure prediction for New York's accident	70
Appendix D: Doubling explosion energy calculations for Allentown accident	71
Appendix E: Doubling explosion energy calculations for New York accident	72
Vita	73

List of Figures

Figure 1 Natural gas pipeline systems (PHMSA, 2014)	7
Figure 2 Cause of incidents for gas distribution system (1994-2013) (PHMSA, 2014)	7
Figure 3 Event Tree Analysis (Muhlbauer, 1996).....	9
Figure 4 VCE in the Pasadena chemical complex [1].....	10
Figure 5 Confined explosion (Bjerketvedt et al. 1997).....	11
Figure 6 Partially confined explosion (Bjerketvedt et al. 1997).....	11
Figure 7 Flash fire [2].....	11
Figure 8 TNT equivalent method chart (DOD, 2008).....	13
Figure 9 TNO multi-energy method chart (BERG, 1985).....	14
Figure 10 Guidance for selecting charge strengths for the TNO method (Crowley, 2004).....	15
Figure 11 BST method chart (Baker et al. 1999).....	16
Figure 12 Former flame speed (Mw) table (Baker et al. 1999).....	16
Figure 13 Updated flame speed (Mw) table (Pierorazio et al. 2005).....	17
Figure 14 Patterns of level of congestion (Pierorazio et al, 2005).....	19
Figure 15 Selected curves for the TNO method (BERG, 1985).....	22
Figure 16 Selected curve for the BST method (Pierorazio et al. 2005).....	22

Figure 17 Allentown's natural gas explosion [3].	24
Figure 18 Locations of involved pipeline, row homes and two collapse homes [4].	24
Figure 19 Fragments distribution around the demolished house [5].	25
Figure 20 Estimated explosion center of Allentown's accident.	26
Figure 21 Selected glass window [3].	27
Figure 22 Reading of house's dimensions from Google earth and location selected glass window.	27
Figure 23 Dimensions of the broken glass window.	28
Figure 24 NFL of a glass window with four sides simply supported (ASTM E1300-12a).	29
Figure 25 Incidence's angle of shock front relative to building wall (DOD, 2008).	29
Figure 26 Reflected pressure coefficient versus angle of incidence (DOD, 2008).	30
Figure 27 Angle of incident of the broken glass window.	30
Figure 28 VCE characteristic by TNO multienergy method (BERG, 1985).	31
Figure 29 VCE characteristic by BST method (Pierorazio et al. 2005).	34
Figure 30 Incident pressure for both flame speeds.	36

Figure 33 Parts of wood flied from the exploded house [3].	38
Figure 34 Estimated distances of the flied wood’s parts.....	39
Figure 35 The demolished houses in Allentown’s accident [6].....	41
Figure 36 Locations and type of damage within 93 to 185 ft from blast center [7].	42
Figure 37 Location of the analyzed building at 450 ft from blast center.	44
Figure 38 West elevation of the building (Benesch, 2011).....	44
Figure 39 Debris distribution of NY's explosion [8].	46
Figure 40 Blast center (BC) and selected glass window locations	47
Figure 41 Dimensions of selected glass window.....	48
Figure 42 NFL for the selected glass window (ASTM E1300-12a, 2012).	48
Figure 43 Associated damage between 30 to 250 ft [9]	53
Figure 44 Associated damage between beyond 250 ft	54
Figure 45 Locations and angle of selected glass windows	56
Figure 46 Selected glass windows. (A) [9]	56
Figure 47 Location and distance of projectile debris [10]	57
Figure 48 Growing area of buildings damage for Allentown accident (Pso =5 psi)	59

Figure 49 Growing area of windows damage for Allentown accident ($P_{so}=0.3$ psi)

.....59

Figure 50 Growing area of buildings damage for Harlem accident ($P_{so} =5.0$ psi)

.....60

Figure 51 Growing area of windows damage for Harlem accident ($P_{so} =0.3$ psi)60

List of Tables

Table 1: Accidental gas explosions (Parfomak, 2013).....	6
Table 2 Congestion levels (Pierorazio et al. 2005).....	19
Table 3 Selected case studies for both methods.....	21
Table 4 Predicted pressure and incident's damage for various distances (TNO method).....	32
Table 5 Incident pressure for both curves of the TNO method.....	33
Table 6 Predicted pressure and incident's damage for various distances (BST method).....	35
Table 7 Incident pressure for both case studies.....	36
Table 8 Reflected pressure between BC to 10 ft.....	38
Table 9 Range of incident pressure within 20 ft.....	40
Table 10 Type of damage when incident pressure more than 3.0 psi.†.....	40
Table 11 Type of damage when incident pressure between 0.23 and 3.0 psi. †....	43
Table 12 Predicted pressure for various distances (TNO method).....	49
Table 13 Predicted pressure for various distances (BST method).....	50
Table 14 Range of incident pressure within 30 ft.....	51
Table 15 Reflected and non-factored load for selected glass windows.....	55
Table 16 Reflected pressure between BC to 10 ft.....	57

Table 17 Distances of real and assumed explosion energy for selected Pso
(Allentown).....59

Table 18 Distances of real and assumed explosion energy for selected Pso60

1. Abstract

Nearly half a million miles of pipeline transport hazardous fluids around the United States. The potential for the release of flammable fluids poses a momentous hazard for the surrounding areas. Of particular concern to our built infrastructure is the accidental leakage and detonation of natural gas pipelines. Two Natural Gas (NG) leakage accidents are examined in detail. This includes the 2011 explosion in Allentown, PA and the 2014 explosion in Harlem, New York. The study consisted of prediction of the incident pressure generated by the NG explosion which can be used to create appropriate safety guidelines and suitable structural design. Two widely used methods: (1) the TNO¹ method and (2) the Baker-Strehlow-Tang method are utilized to predict the overpressure generated by the NG vapor cloud explosion (VCE). The observed damage to surrounding buildings is correlated with known window breakage strengths and is used to verify the accuracy of the computed overpressure from these methods for the two case studies. The resulting overpressure values are further verified using the distances that debris was thrown from the explosion site. The Modified Bernoulli Equation (MBE) is utilized for this calculation. The methods are shown to provide an accurate estimate of the initial detonation energy. Utilizing this approach, the effect of doubling the explosion energy of VCE on the surrounding buildings in Allentown and Harlem is examined. This increase results in a 67% and 64% increase to severe damage to brick buildings and a 66% and 44% increase in the region over which window damage is likely to occur, respectively.

¹ The Netherlands Organization for Applied Scientific Research (TNO)

2. Introduction

Accidental leakage of flammable fluids could generate overpressure, after ignition, which results in a potential risk of death or injury and damage to structures. In fact, more than half of the total fatalities and injuries related to pipeline accidents are associated with gas distribution systems (PHMSA, 2014). Accidental explosions from natural gas leakage have become a common occurrence in residential U.S. neighborhoods. These events lead to significant damage to neighborhoods and death and injury to the residents. For instance, the 2011 event in Allentown, PA and the 2014 event in Harlem, New York resulted in the loss of thirteen people and injury to over seventy people.

To address the issue of residential explosions a study is conducted to predict the overpressure of the natural gas detonations and is used to aid in creating appropriate safety guidelines and suitable structural designs. Two methods to predict these type of explosions (vapor cloud explosions) are used. This includes the TNO multienergy and Baker-Strehlow-Tang (BST) method as applied to the Allentown and Harlem events. The damage from the predicted overpressure is compared with the actual damage of Allentown and New York explosion and found to correlate well. In addition, the load resistance of building's glass window provided by ASTM E1300-12a (2012) is compared with incident pressure from the explosions. Projectile debris from the events is analyzed by the Modified Bernoulli Equation (MBE) to further verify the predicted overpressure values from the TNO and BST methods. The verified approaches are extrapolated to

alternate scenarios where larger amounts of gas is collected prior to detonation and the effects of this on the damage is presented.

3. Natural Gas Accidents

Around 300,000 miles of gas pipelines connect the U.S. These pipelines network feed over 66 million customers (Parfomak, 2013). While the utilitarian need of the transported contents is vital for society, many pipelines contain volatile, flammable or toxic materials which pose the potential for public injury and environmental damage. Pipeline systems in the U.S. include hazardous liquid, and gas transmission, gas gathering, and gas distribution systems. Between 2007 through 2011 there were on average 14 fatalities and 64 injuries per year from all pipeline systems; of those numbers over half (64% of fatalities and 67% of injuries) were directly associated with gas distribution pipelines (PHMSA, 2014).

Accidental distribution pipeline leakage has been associated with material weld and equipment failures, excavation damage, corrosion, other outside force damage (e.g. fire or explosion), operator error, and other causes. Moreover, natural events including earthquakes and floods pose a major risk for pipeline damage. The percentage of each accident's cause from 1994 to 2013 is presented in Figure 2 where damage due to excavation, outside force, and other causes possess higher percentages than other causes (PHMSA, 2014).

Pipeline distribution systems consists of low pressure and high pressure systems. The pressure of gas in low pressure distribution system is common in residential and commercial connection and can reach a maximum value of 2 psi. High pressure distribution systems operate at pressures above 2 psi (ASME B31.8, 2003).

Maintenance for distribution piping system is a significant function during the pipeline operation stage. Maintenance function includes four factors which are patrolling of pipeline at required conditions (e.g. during construction activity), providing leakage survey (e.g. addressing the source of leakage), leakage investigation and action, and abandoning, disconnecting, and reinstating the inactive facility. Addressing the source of leakage can be achieved by several tests including pressure drop test, bubble leakage test, and ultrasonic leakage test (ASME B31.8, 2003).

For distribution piping system, the average installing year for the NG pipelines that caused incidents between 2004 and 2014 is 1971; in addition, total number of accidents from all type of gas distribution system is 1378 accidents while 1345 (98 %) accidents were caused by the NG pipelines only (PHMSA, 2014).

The NG pipeline transportation systems consist of three types: gathering system, transmission system, and distribution system (Figure 1). Gathering pipelines collect raw NG from wells and transfer it to gas processing and treatment plant. Transmission pipelines transport the NG from gas processing and treatment plant to storage, directed served customers (e.g. electric power generation station), and/or city gate. Distribution pipelines distribute the NG to residential and business building by mains and service lines. Diameter of NG pipeline systems ranges from 2 to 42 inches, excluding service lines where it varies from 0.5 to 2 inches (PHMSA, 2014).

This study focuses on the issue of accidental leakage and explosion related to natural gas pipelines in residential and commercial buildings. This is a prevalent issue in the U.S. as noted by some of the recent severe accidents summarized in Table 1. To

investigate this issue more closely, the Allentown and New York events are examined in detail.

Table 1: Accidental gas explosions (Parfomak, 2013).

Location	Year	Type of building ²	Accident type	Fatalities	Injuries
Flixborough, UK ³	1974	Commercial	Leak-explosion-fire	28	36+
Pasadena, TX ⁴	1989	Commercial	Leak-explosion-fire	23	130+
Bellingham, WA	1999	Open area	Leak-explosion- fire	3	8
Carlsbad, NM	2000	Open area	Leak-explosion-fire	12	None
San Bruno, CA	2010	Residential	Leak-explosion-fire	8	60
Allentown, PA	2011	Residential	Leak-explosion-fire	5	NA
Springfield, MA	2012	Commercial	Leak-explosion-fire	None	21
New York, NY ⁵	2014	Residential	Leak-explosion-fire- progressive collapse	8	70+

² This part has been added by the author.

³ <http://www.hse.gov.uk/comah/sragtech/caseflixboroug74.htm>

⁴ The Pasadena accident information were collected from (U.S. Department of Labor, 1990)

⁵ Siff & Russo, 2014

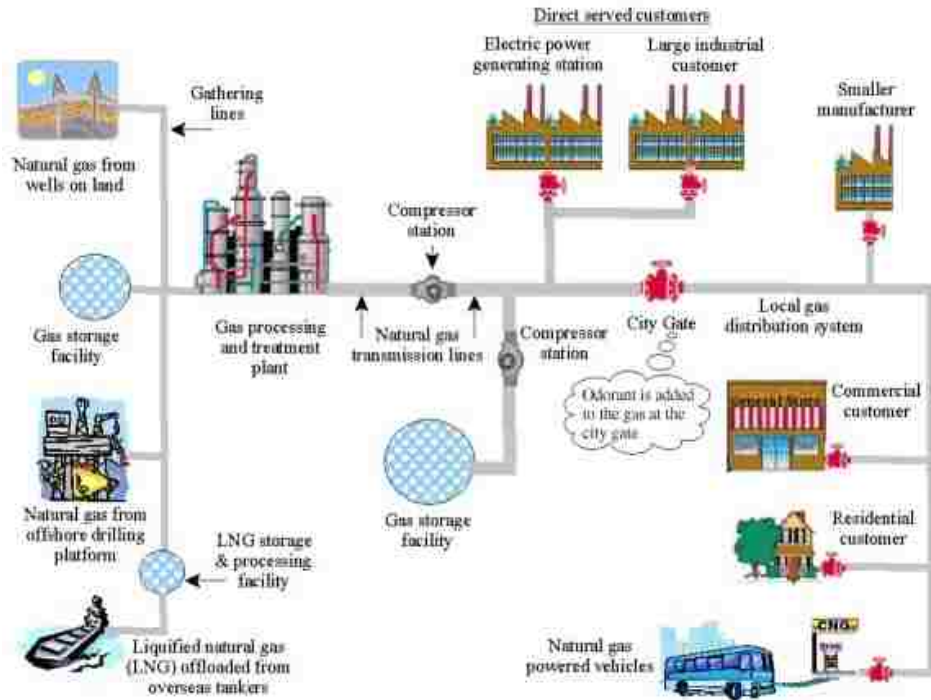


Figure 1 Natural gas pipeline systems (PHMSA, 2014)

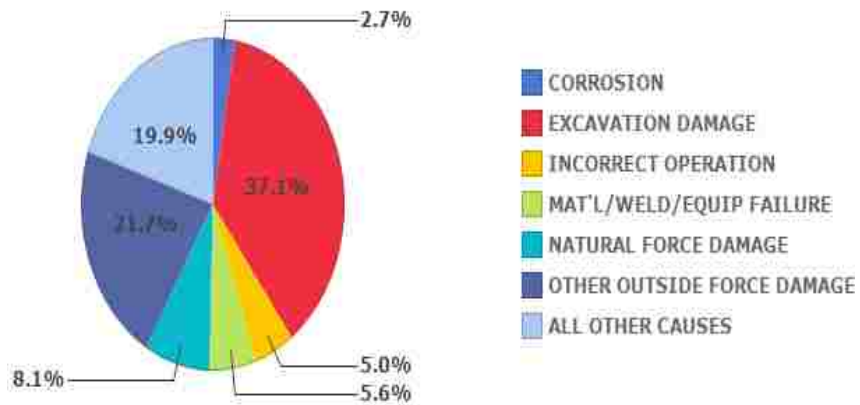


Figure 2 Cause of incidents for gas distribution system (1994-2013) (PHMSA, 2014)

4. Possible Scenarios of a Fuel Gas Release

Accidental release of flammable gas poses a significant hazard for structures and people in the vicinity of the release. The amount and type of damage generated is dependent on what happens to the gas which in turn is dependent on how the gas is confined. A standard approach for determining the final outcome of the gas has been developed by Muhlbauer (1996). The approach consists of an Event Tree Analysis (Figure 3) where each final outcome is related to significant factors. These factors are time of ignition and degree of confinement of the gas.

Detonation or deflagration of the accidental gas release occurs when it is immediately ignited in a confined space. Detonation consists of a combustion wave that propagates through the gas at supersonic speeds while deflagration propagates at subsonic speed. If the space is unconfined the result would be a fireball or jet fire which is dependent on the nature of the release.

For cases where ignition of the gas is delayed, a confined vapor cloud explosion (CVCE) or flash fire could occur. As is apparent from the name a CVCE occurs if ignition occurs in a confined space while a flash fire would occur in an unconfined space. A CVCE generates a high pressure wave (e.g. deflagration or detonation) which can generate significant demand on structures and occupants. A flash fire in contrast consists of a low velocity propagation of the combustion wave through the gas that generates negligible overpressure. These cases are related to the mixing of fuel release gas with the

air at time of ignition. Variation in gas concentration will produce different flammable limits and different combustion characteristics.

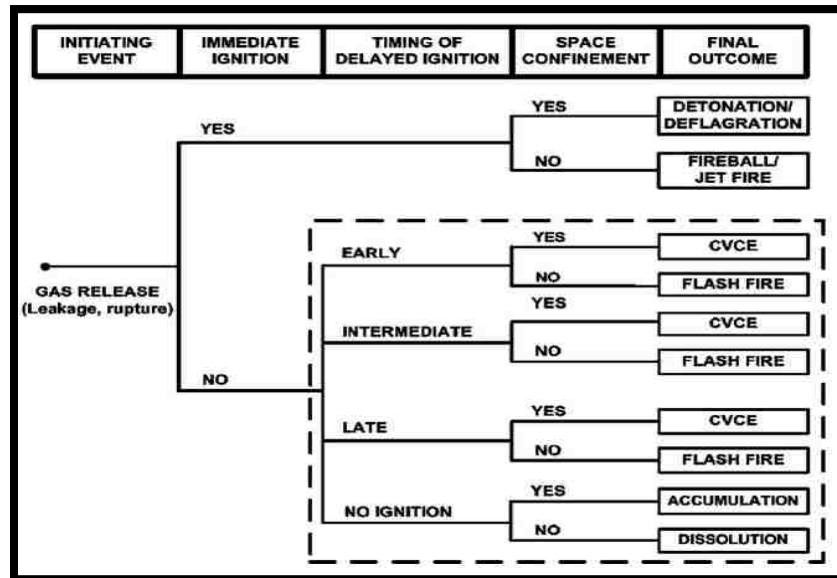


Figure 3 Event Tree Analysis (Muhlbauer, 1996).

5. Vapor cloud explosion (VCE)

When an ignition takes place in a cloud of flammable vapor (e.g. natural gas) the flame speed will accelerate during combustion generating an explosion and overpressure, this is known as a vapor cloud explosion or VCE (Figure 4). The effect of the explosion depends on the containment of the area where the explosion occurs. Gas explosions are commonly categorized as: (i) Confined vapor cloud explosion (CVCE) (e.g. within vessels), (ii) Partially confined vapor cloud explosion (e.g. in a building), and (iii) Unconfined vapor cloud explosion (UVCE) (e.g. when a combustible gas ignited in open atmosphere (Bjerketvedt et al. 1997). A CVCE and partially CVCE may initiate under the same circumstances and can lead to considerable different demands. Figure 5 and Figure 6 show the CVCE and the partially CVCE. According to Nolan (2011), enough congestion or turbulence in air is required in order for UVCE to occur. For low congestion, a UVCE would result in a flash fire (Figure 7).



Figure 4 VCE in the Pasadena chemical complex [1].

[1] <http://www.fireworld.com/Archives/tabid/93/articleType/ArticleView/articleId/87013/WRONG-PASADENA.aspx>

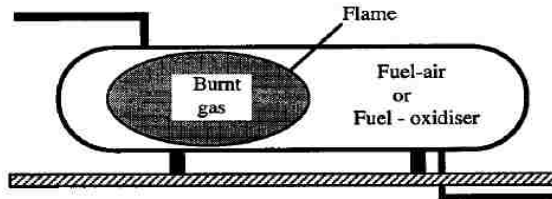


Figure 5 Confined explosion (Bjerketvedt et al. 1997)

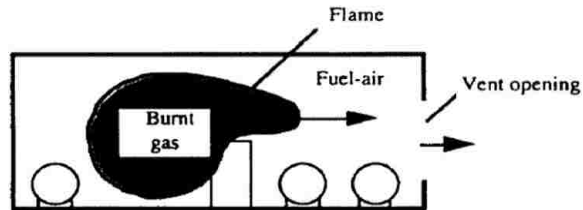


Figure 6 Partially confined explosion (Bjerketvedt et al. 1997)



Figure 7 Flash fire [2]

[2] <http://www.youtube.com/watch?v=3u9UyKNhuFI>

5.1. Demand Estimation Procedures for VCE

A VCE accident occurred in Flixborough, U.K. in 1974. Large quantities of cyclohexane leaked and formed a flammable mixture which subsequently ignited to produce a massive VCE. As mentioned earlier, the VCE killed 28 workers and injured more than 36. After this explosion, several prediction methods were developed to analyze VCEs and to aid in creating appropriate safety guidelines and suitable structural design (Lenoir, E. M. and Davenport, J. A., 1992). The three most widely used methods to predict the blast demands generated from a VCE, are the TNT equivalent method, the TNO multienergy method, and the Baker-Strehlow-Tang (BST) method. Each method provides a non-dimensionalized blast curve to predict overpressure given the source, amount of energy generated, and the standoff distance. The number and type of curves vary for each method (Pierorazio et al. 2005).

5.1.1. TNT equivalent method

The TNT equivalent method equates the energy released into an equivalent amount of TNT. Given the energy of the VCE an equivalent weight of TNT is determined. This value along with the effective standoff distance R is used to determine the incident and reflected pressures, P_{so} and P_r , (Figure 8). The complication in the method lies in the determination of the VCE energy and properly equating it to an equivalent weight of TNT. The combustion energy of the VCE is based on confinement shape, congestion level and fuel reactivity that can be difficult to assess. Hence, the method is no longer widely used.

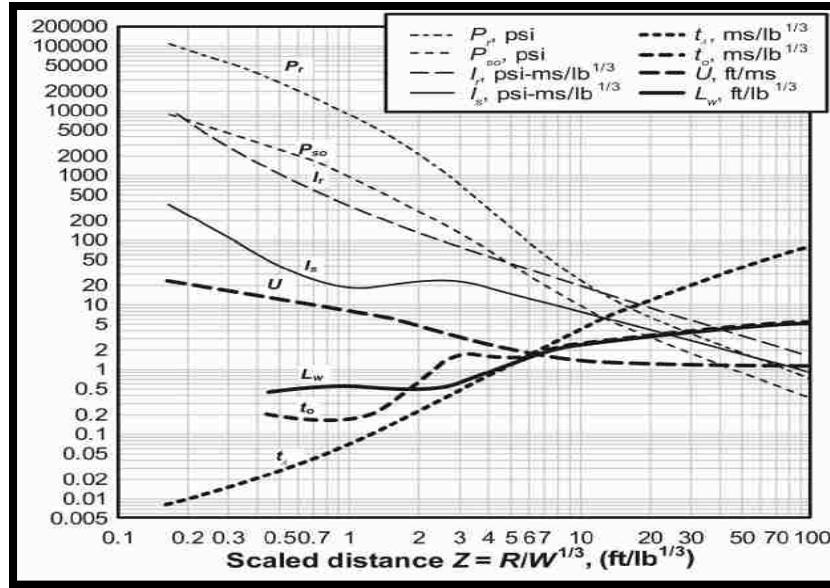


Figure 8 TNT equivalent method chart (DOD, 2008).

5.1.2. TNO multi-energy method.

The TNO approach categorizes the severity of the explosion and provides a method to determine the blast pressures as a function of the scaled distance (Figure 9). Ten categories are used for the severity of the VCE. This ranges from curve 1 (insignificant strength) to curve 10 (gaseous detonations). Selecting a certain curve is based on the potential severity or flame speed of the explosion. In case of partially confinement, however, a conservative estimate provided by choosing a curve higher than number 6 or 7 (BERG, 1985). In addition, Crowley (2004) provides a table to assist in selecting the appropriate curve based on confinement shape, congestion level and fuel reactivity (explained later) (Figure 10). Knowing the curve category and the scaled distance, previously defined, the dimensionless maximum side on pressure can be determined. This in turn can be used to compute the combustion energy as shown in equation 1 and equation 2.

Figure 9 illustrates the pressure estimation curves developed for the TNO method.

The terms in these formulas explained below:

$$\bar{\Delta P}_s = \frac{P - P_o}{P_o} \quad (1)$$

$$\bar{R} = \frac{R}{(E/P_o)^{1/3}} \quad (2)$$

Where, $\bar{\Delta P}_s$ is dimensionless maximum side on overpressure; \bar{R} is combustion energy-scaled distance; P_o is atmospheric pressure; P is absolute pressure (gauge pressure + atmospheric pressure); R is distance from cloud center; and E is combustion energy released.

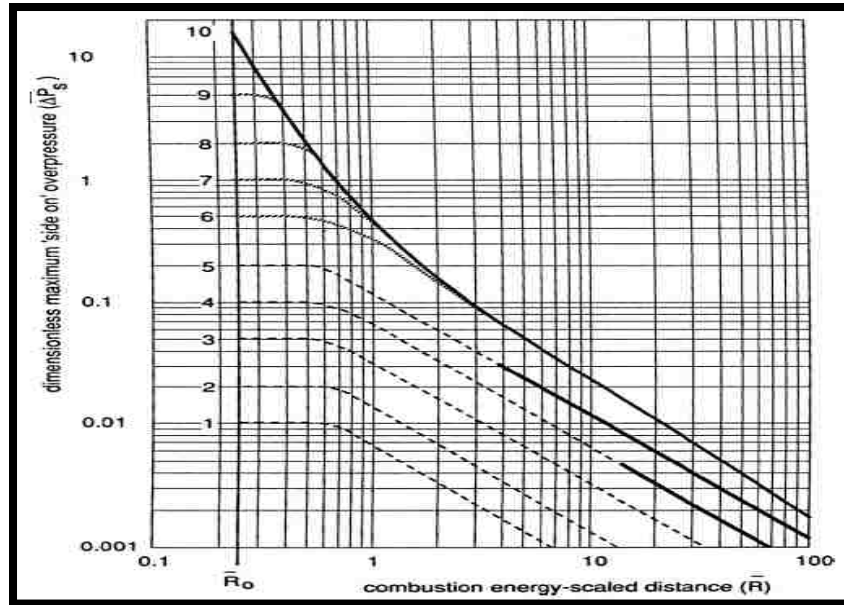


Figure 9 TNO multi-energy method chart (BERG, 1985).

Type of Flame Expansion ²	Mixture Reactivity ³	Obstacle Density ⁴		
		High	Medium	Low
2-D	High	DDT	DDT	6
	Medium	8 - 9	6 - 7	5 - 6
	Low	6 - 7	5 - 6	2 - 3
2.5-D	High	DDT	DDT	5 - 6
	Medium	7 - 8	6	4 - 5
	Low	5 - 6	5	3
3-D	High	DDT	DDT	5
	Medium	5 - 6	5 - 6	2 - 3
	Low	5	4	1

Figure 10 Guidance for selecting charge strengths for the TNO method (Crowley, 2004).

5.1.3. The Baker-Strehlow-Tang (BST) method.

The BST blast load prediction methodology uses flame speed to measure the severity of VCE. The method contains a family of curves developed based on the flame speed (Mach number) of combustion energy (Figure 11). Mach number represents a ratio of speed of an object to the speed of sound in a surrounding environment. Two definitions for flame speed (M_w and M_f) are presented in this method. A relationship between M_w and M_f has been developed by (M. J. Tang and Q. A. Baker, 1999). According to Baker M. J. (1999) " M_f is apparent flame Mach number relative to a fixed observer (flame speed)." Figure 11 illustrates the ranging of flame speed (M_f) for each curve, from slow deflagration to detonation shock fronts of propagated strength. The BST method developed a table to assist in selecting the appropriate curve where the values in this table are in Mach number M_w (Baker, Tang, Scheler, & Sliva, 1999) (Figure 12). The table was updated in 2005 and represents values of M_w as well (Figure 13) (Pierorazio et al. 2005). Choosing flame speed is influenced by degree of confinement, fuel reactivity and obstacle density (congestion level). These factors will be explained

below. The terms in Figure 11 are, P_o is atmospheric pressure; P is absolute pressure (gauge pressure + atmospheric pressure); R is distance from cloud center; and E is combustion energy released.

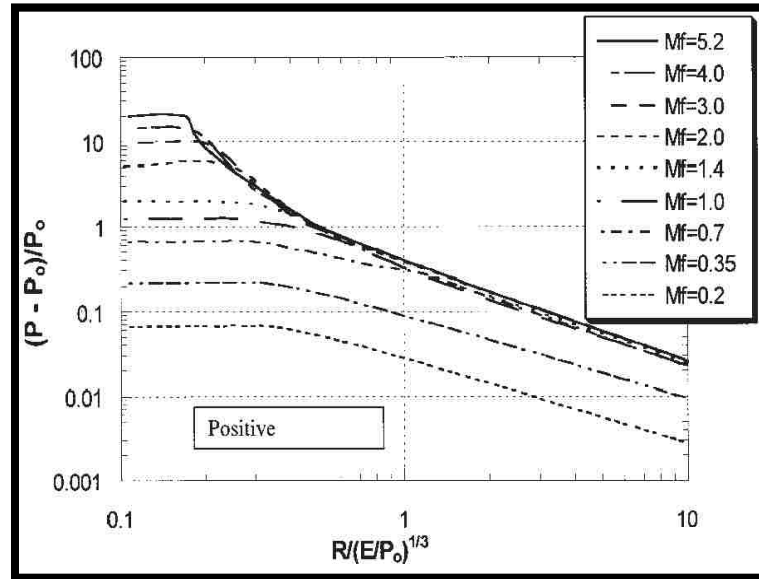


Figure 11 BST method chart (Baker et al. 1999).

		OBSTACLE DENSITY		
		High	Medium	Low
1D FLAME EXPANSION	High	5.2	5.2	5.2
	Medium	2.265	1.765	1.029
	Low	2.265	1.029	0.294
2D	High	1.765	1.029	0.588
	Medium	1.235	0.662	0.118
	Low	0.662	0.471	0.079
3D	High	0.588	0.153	0.071
	Medium	0.206	0.100	0.037
	Low	0.147	0.100	0.037

Figure 12 Former flame speed (Mw) table (Baker et al. 1999)

Confinement	Reactivity	Congestion		
		Low	Medium	High
2-D	High	0.59	DDT	DDT
	Medium	0.47	0.66	1.6
	Low	0.079	0.47	0.66
2.5-D	High	0.47	DDT	DDT
	Medium	0.29	0.55	1.0
	Low	0.053	0.35	0.50
3-D	High	0.36	DDT	DDT
	Medium	0.11	0.44	0.50
	Low	0.026	0.23	0.34

Figure 13 Updated flame speed (Mw) table (Pierorazio et al. 2005).

5.1.3.1 Degree of confinement

The degree of confinement must be determined in order to select the appropriate flame speed of a VCE. Preventing a flame front from freely expanding is known as confinement. Three cases of confinements can be defined as 3D, 2D and 1D confinement. In addition, 2.5D is case of confinement that consists of an average between 2D and 3D values. The three degrees of confinement are explained below:

- 3D confinement: means flame expanding freely in three dimensions. (e.g. flame in open area).
- 2.5D case considered when the confinement is made of frangible panel (e.g. compressor shelters with lightweight roofs).
- 2D confinement: means flame expanding freely in two dimensions. (e.g. flame beneath a solid deck).
- 1D confinement: means flame expanding freely in one dimension. (e.g. flame in a tube).

5.1.3.2 Fuel reactivity

The fuel reactivity must also be determined to select the appropriate flame speed of a VCE. According to Melton, T. A. and Marx, J. D. (2008), "Fuel reactivity is a measure of the propensity of the flame front in a given flammable mixture to accelerate and create overpressures or potentially undergo a deflagration to detonation transition (DDT)". Reactivity is classified as low, average and high (Zeeuwen, J.P, and B.J. Wickema, 1978). Most of materials are of average reactivity; methane, carbon monoxide and NG are classified as low reactivity; hydrogen, acetylene, ethylene oxide and propylene oxide are considered to be highly reactive (Crowley, 2004).

5.1.3.3 Congestion level

The amount of congestion in the vicinity of the gas leakage impacts the explosive event. When the flame accelerates through an array of obstacles the congestion level of the obstacles must be determined. Blockage ratio and pitch are the two significant factors for determining level of congestion. Blockage ratio equals to area blocked by obstacle over the total cross section area of the obstacle. Pitch defined as the distance between blockage rows. Three levels of congestion were defined which are low, medium, and high congestion (Figure 14); in addition, pitch to diameter and area to blockage ratios are described in more depth by Pierorazio et al. (2005) and illustrated in Table 2. When the blockage ratio is high, the flame speed and consequently, overpressure of the VCE will be high (Baker et al. 1999).

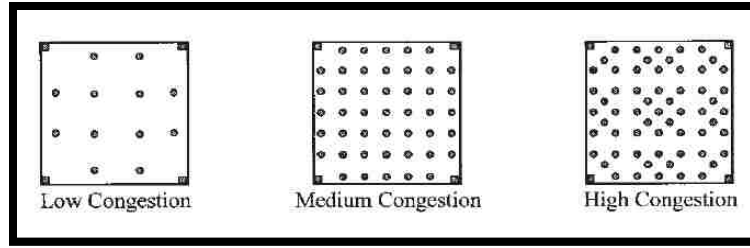


Figure 14 Patterns of level of congestion (Pierorazio et al, 2005)

Table 2 Congestion levels (Pierorazio et al. 2005)

Congestion level	Pitch to diameter ratio	Area blockage ratio (%)
Low	7.6	13
Medium	4.3	23
High	3.1	23

6. Estimated scenarios for both accidents (Allentown and Harlem)

Selecting the appropriate curve in the VCE is influenced by confinement degree, fuel reactivity and congestion level (explained earlier). Reactivity of the NG was founded to be low (Crowley, 2004). However, the actual level of congestion and the degree of confinement were difficult to determine as a result of the buildings being demolished by the explosions. Different congestion and confinement scenarios were developed and analyzed below.

Three different scenarios were considered in this paper. The NG explosions in Allentown and Harlem exhibited debris (e.g. bricks and wood) around the destroyed building. These effects result in a categorization of frangible confinement (Figure 17 and Figure 37). A frangible panel is considered to provide 2.5D degrees of confinement according to Pierorazio et al. (2005) and therefore is selected for this study. In addition, a 2D degree of confinement was assumed representing a case where the floors in the demolished buildings were not frangible which would prevent the flame front from propagating through the floors and resulting in expansion in two dimensions only. The amount of congestion within each structure was not known since both buildings were demolished. The congestion level was estimated as medium and high based typical furnishings in the region. Low congestion was ruled out based on the observed damage. For low congestion the damage curves for the TNO method (curve no. 2 and 3) and the BST method (Mf 0.053 and 0.079) do not correlate with observed damage. Therefore, low congestion was not examined.

The selected factors of confinement, congestion and reactivity are used with Figure 10 and Figure 13 to examine the demands generated from the three scenarios for each method (the TNO and the BST). The results are provided in Table 3. In addition, the selected strength curves for the TNO method and the selected Mach number curves for the BST method are shown in Figure 15 and Figure 16. The selected curves in the TNO method include curve numbers 6 and 7. Curve number 5 was not selected since the maximum overpressure for this curve (2.94 psi) would not cause severe damage. In addition, it is recommended by (BERG 1985) to use curve higher than number 6 or 7 in case of partial confinement (e.g. residential building). The presented curves in Figure 16 based on M_f values. However, the curve of M_f 0.66 and M_f 0.93 are not provided in Figure 16; therefore, interpolation was used to calculate overpressure values.

Table 3 Selected case studies for both methods.

Cases	Confinement	Reactivity	Congestion	The BST		The TNO
				Mw	Mf	Curve no.
1	2.5D	Low	High	0.50	0.7	5-6
2	2D	Low	Medium	0.47	0.66	5-6
3	2D	Low	High	0.66	0.93	6-7

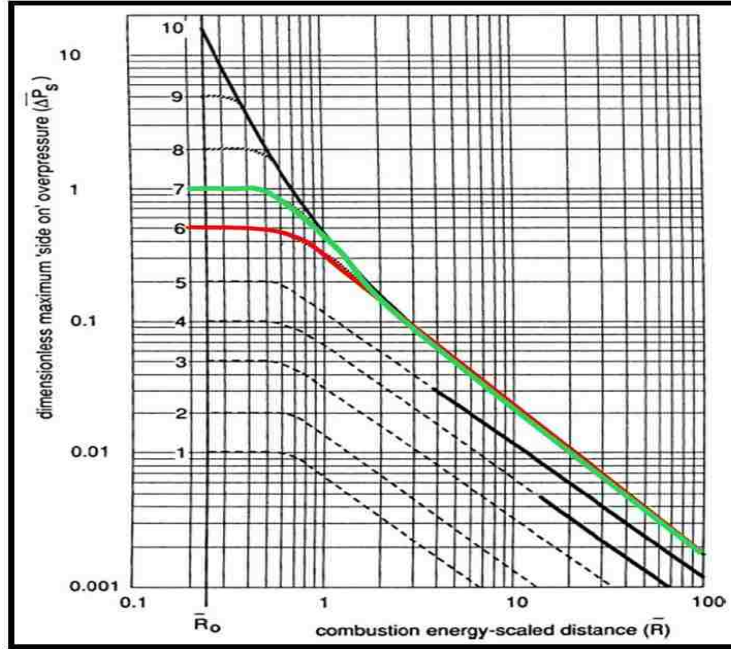


Figure 15 Selected curves for the TNO method (BERG, 1985).

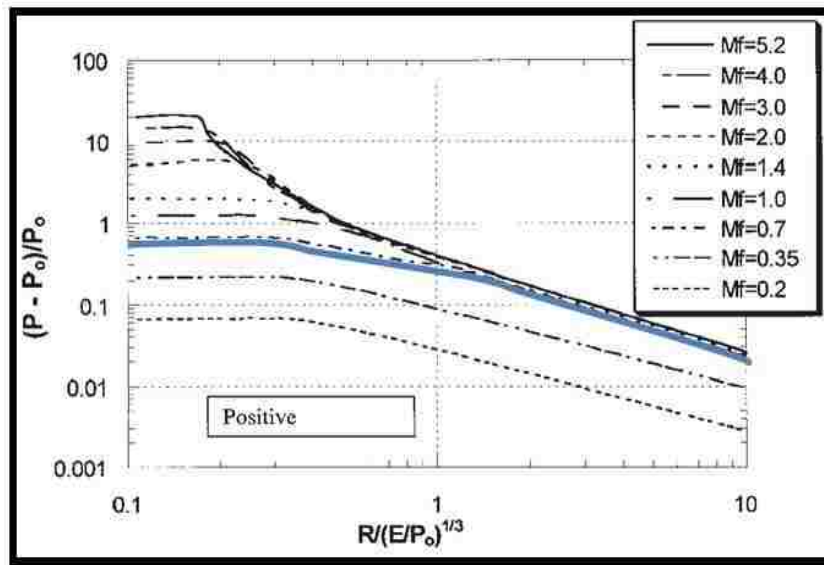


Figure 16 Selected curve for the BST method (Pierorazio et al. 2005).

7. Allentown case study

A case study of the February, 9th, 2011 event in Allentown, PA is conducted. Two homes of an eight unit row house were destroyed by the event (Figure 17). The remaining six units were not salvageable. Five people died at the event; two from blunt force injuries from the explosion, one from possible asphyxiation or being crushed, one from carbon monoxide poisoning. The cause of the last fatality was not determined. A dozen people were injured and more than 350 people evacuated (Sheehan et al. 2011).

The homes in the area were supplied by a 12 inch diameter low pressure natural gas pipeline. The maximum value of low pressure distribution system is 2 psi (ASME B31.8, 2003). The pipeline was identified as cast-iron (Lehman, 2011) and was installed in 1928, supported on brick and backfilled with asphalt overlay. A crack was identified in the pavement above the pipe and a crack was located in pipe at the brick support (Richard Young, personal communication, 2013). According to McEvoy (2012), the cracked pipe was identified as the official source of the gas leak. Figure 18 shows locations of the collapsed and the unsalvageable of row homes and location and excavation for replacement of the involved pipeline.

Based on the observations of damage to the structures and the associated news footage the Allentown event is likely due to a partially CVCE. From the images taken after the event it is clear that immediate ignition of the natural gas did not take place. The debris spread radiating from the end row home is indicative of an internal confined detonation (Figure 19). Due to the significant amount of damage it is likely that the early, intermediate or late ignition of the gas had occurred. While it is only speculation,

the fact that an elderly couple, with potentially reduced olfactory senses, lived in the end row home could be a contributing factor to the undetected accumulation.



Figure 17 Allentown's natural gas explosion [3].

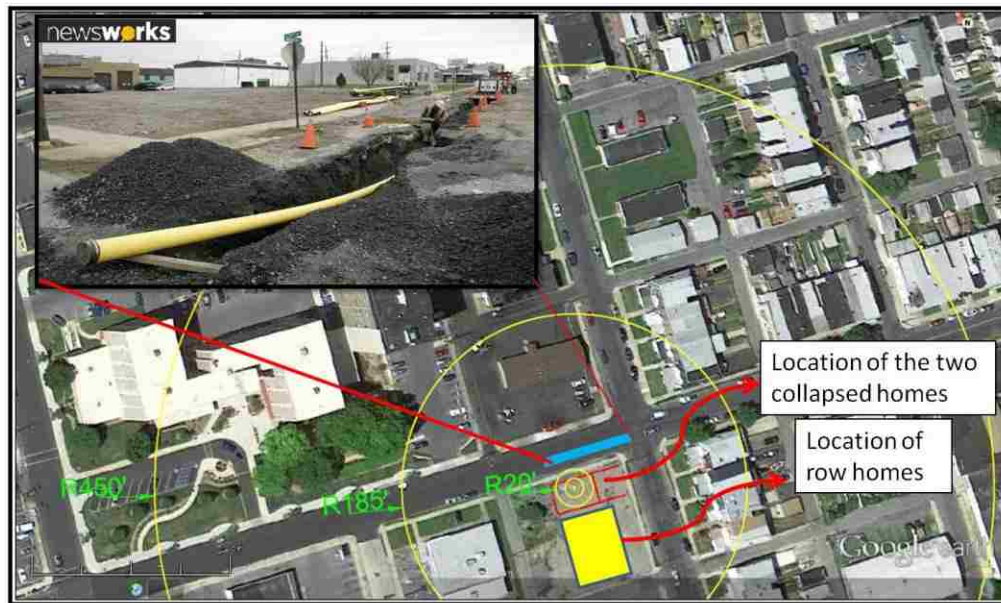


Figure 18 Locations of involved pipeline, row homes and two collapse homes [4].

[3] <http://www.mcall.com/news/breaking/mc-allentown-explosion-aerial-photos-014,0,113077.photo>

[4] <http://www.newsworks.org/index.php/local/the-latest/62926-new-pipeline-will-carry-natural-gas-liquids-across-state-to-delaware-county-refinery->

To assess the energy of the explosion, overpressure of the VCE is used. This requires the determination of the cloud center and a means of determining the energy of the explosion. The energy is estimated from observed window breakage. The process for determining these points are summarized in this section.

7.1. Center of Blast

Locating the center of VCE is an important factor to predict the overpressure of the NG explosion. Therefore, estimation was developed to position the cloud center based on the distribution of fragments around the end of the house on row as mentioned earlier (Figure 19). The location of the center of blast was assumed to be in the center of the end house and it is shown in Figure 20 and Figure 22.



Figure 19 Fragments distribution around the demolished house [5].

[5] http://www.lehighvalleylive.com/joe-owens/index.ssf/2011/02/allentown_explosion_requires_s.html



Figure 20 Estimated explosion center of Allentown's accident.

7.2. *The broken glass window*

7.2.1. **Dimensions of the broken glass window**

Several photos of Allentown's event demonstrate the resulting damage from the accelerated waves of the NG explosion, including two collapsed houses and glass windows that were blown out. In order to predict the pressure value of the incident, a broken glass window was selected to measure the explosion energy (Figure 21). Based on event's photos, the selected window has the maximum distance from the cloud center, which indicates that the explosion energy that will be calculated from this window is the highest energy that can be reached out of all the other broken domestic glass windows in Allentown's accident.



Figure 21 Selected glass window [3].

To determine the breakage load for the selected glass window, the dimensions of the window must first be determined. Figure 22 shows the measurement of the length of the elevation side of the house (45 ft) where the selected glass window is located. By scaling the photo in AutoCAD, this length was adjusted to the photo that was taken from Google maps (Figure 23) and then dimensions of the selected glass window were determined. As a result, the dimensions of the window were found to be approximately 34 inches long and 24 inches wide. In addition, the window's thickness is assumed as 1/8 inch.



Figure 22 Reading of house's dimensions from Google earth and location selected glass window.

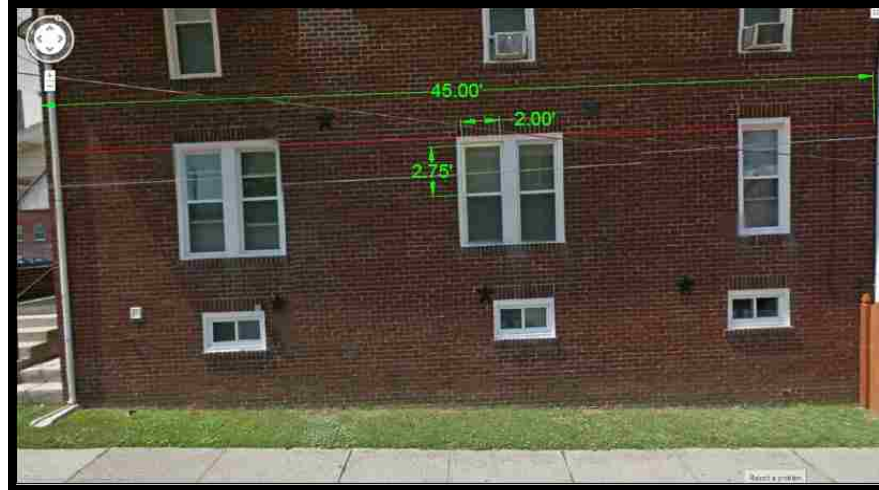


Figure 23 Dimensions of the broken glass window.

7.2.2. Failure load of a glass window.

A glass window must be designed to resist several types of loads, including the exposed uniform lateral load (e.g. wind load). The maximum uniform lateral load which a glass window is able to withstand is called Load Resistance (LR) (ASTM E1300-12a, 2012). The type of glass window involved in Allentown's explosion is assumed to be annealed glass; in addition, short duration load was assumed for the selected windows; as a result, the LR value equals the Non-Factored Load (NFL); charts were developed to determine NFL for various glass windows' thicknesses by importing the long and short dimension of a glass window (ASTM E1300-12a, 2012). Since the thickness of the glass window was assumed as 1/8 inch, a chart was selected and long and short dimension of the window were entered (Figure 24). Hence, NFL pressure equals to 0.48 psi (3.3 kPa). This pressure is the reference point to predict other pressure values in different locations for Allentown's case study by using the TNO and BST methods.

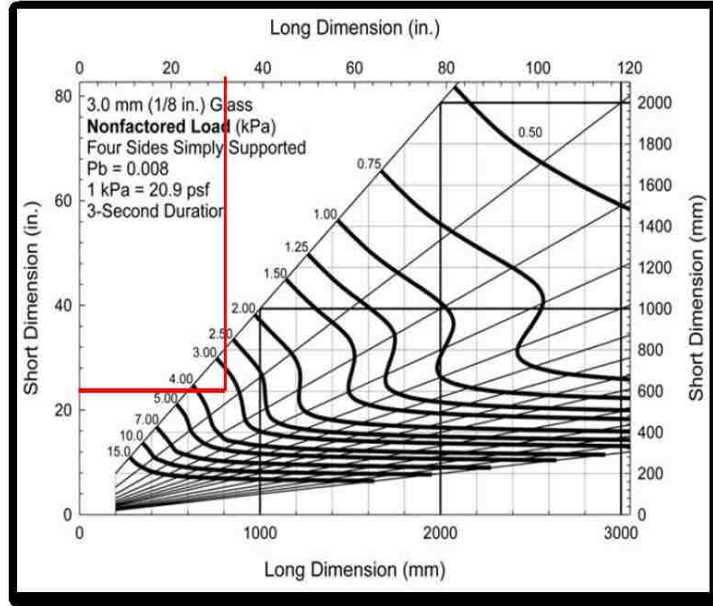


Figure 24 NFL of a glass window with four sides simply supported (ASTM E1300-12a).

7.3. Reflected pressure (P_{ra}) and incident pressure (P_{so}):

When a shock wave propagation strikes a structure surface, the value of reflected pressure (P_{ra}) varies based on the angle of incidence (α) between the surface and the direction of shock waves (Figure 25). A relationship between angle of incident and reflection factor (C_{ra}) was developed by UFC 3-340-02 (2008) (Figure 26). Reflection factor is the ratio of reflected pressure to incident pressure (P_{so}).

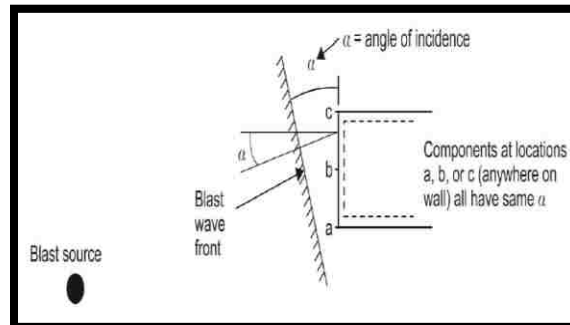


Figure 25 Incidence's angle of shock front relative to building wall (DOD, 2008).

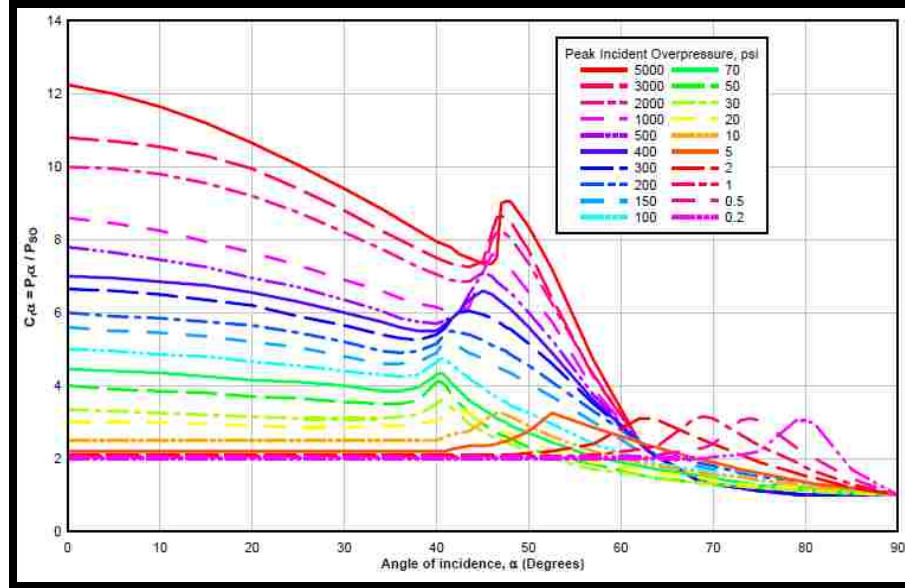


Figure 26 Reflected pressure coefficient versus angle of incidence (DOD, 2008).

Since the broken glass window has an oblique angle (α) from the blast center (Figure 27), the NFL value of 0.48 psi (founded before) represents the reflected pressure. By importing the angle of incident (68°) to Figure 26, as a result, the corresponding reflected pressure coefficient is about 2.1. By dividing the reflected pressure (0.48 psi) by the reflection factor (2.1), as a result, incident pressure at the location of the broken glass window equals 0.23 psi.



Figure 27 Angle of incident of the broken glass window.

7.4. Pressure prediction

7.4.1. Predicting pressure by the TNO method

The TNO curves represent the blast wave properties of VCE as a function of scaled distance. To predict overpressure of VCE accident, the appropriate curve number in the TNO method must be selected. Therefore, curve numbers 6 and 7 were selected previously based on degree of confinement, fuel reactivity, and congestion level. The calculations to predict overpressure for both curves possess the same methodology. Thus, only calculation for curve number 7 provided below.

Since the incident pressure that caused breakage of glass window corresponds to 0.23 psi (calculated before) and atmospheric pressure is assumed as 14.7 psi, then, equation 1 for the y-axis equals 0.016. From Figure 28, a dimensionless maximum side on overpressure of 0.016 corresponds to a combustion energy scaled distance of 14.0. By using equation 2 and since location of glass window (R) was known as 185 ft (explained before), as a result, explosion energy (E) will be equal 4.89E6 ft-lb.

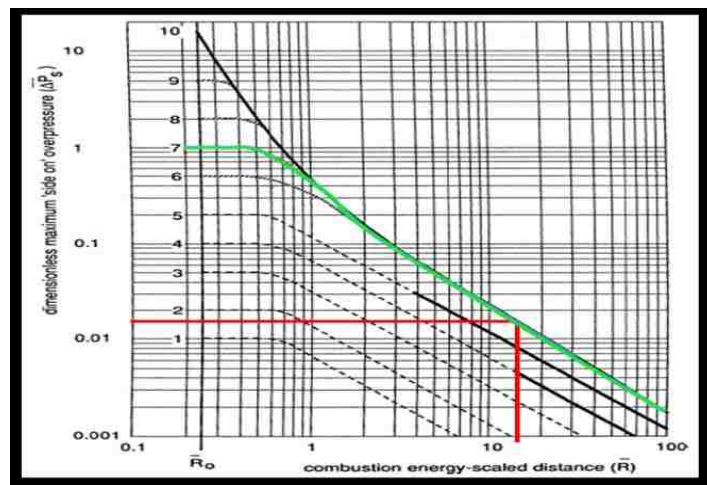


Figure 28 VCE characteristic by TNO multienergy method (BERG, 1985).

To predict overpressure at any location around the cloud center, the calculation only requires selecting a distance (R) from the cloud center since all other variables in equation 2 are known. An example is shown here to predict the overpressure at 20 feet (i.e. locations of the front and back wall of the demolished house) (Figure 20). From equation 2, scaled distance (X-axis) is about 1.51 which corresponds to maximum side on overpressure (Y-axis) of 0.23 (Figure 28). As a result, incident pressure and reflected pressure for zero angle of incident correspond to 3.68 and 8.0 psi, respectively. Predicted overpressures for other locations around blast center are illustrated in Table 4. All calculations of overpressure prediction are developed in appendix A.

Table 4 Predicted pressure and incident's damage for various distances (TNO method).

Damage	Distance from blasting center (ft)	Incident Pressure (psi)	Reflected Pressure* (psi)
Brick wall blown out	10	10.0	25
House demolished	20	3.68	8.0
Painting Shop (broken glass window)	93	0.50	0.79
Roller doors collapsed (front side)	120	0.38	0.76
Roller doors collapsed (back side)	155	0.3	0.3
Glass window breakage (ASTM E1300)	185	0.23	0.48
Bank slightly damaged and large window breakage	450	0.09	0.18

*Reflected pressure coefficient calculations are explained in Appendix B.

Beyond 30 ft from blast center, curves number 6 and 7 merge together which mean both of the curves result in the same overpressure. Therefore, Table 7 illustrated the values of overpressure below 30 ft for both curves.

Table 5 Incident pressure for both curves of the TNO method

Incident pressure (Pso), psi		
R, ft	Curve number	
	6	7
BC	7.4	14.7
10	5.5	10.0
20	3.2	3.68
30	1.9	

7.4.2. Predicting pressure by BST method

The appropriate curves were selected to characterize overpressure of the NG blast in Allentown. Both selected flame speed curves (Mf 0.66, 0.7 and, 0.93) have similar procedures in calculating overpressure for Allentown's accident. Thus, only the Mf 0.7 case study will be explained below.

7.4.2.1 Explosion energy (E) developing and pressure prediction

Since incident pressure (gauge pressure) at the location of broken glass window was estimated as 0.23 psi and atmospheric pressure was assumed as 14.7 psi, then, equation 1 for Y-axis corresponds to 0.016. Therefore, X-axis equals 15. By using equation 2 and since R and P_o were known, as a result, explosion energy (E) equals 3.97E6 ft-lb (Figure 29).

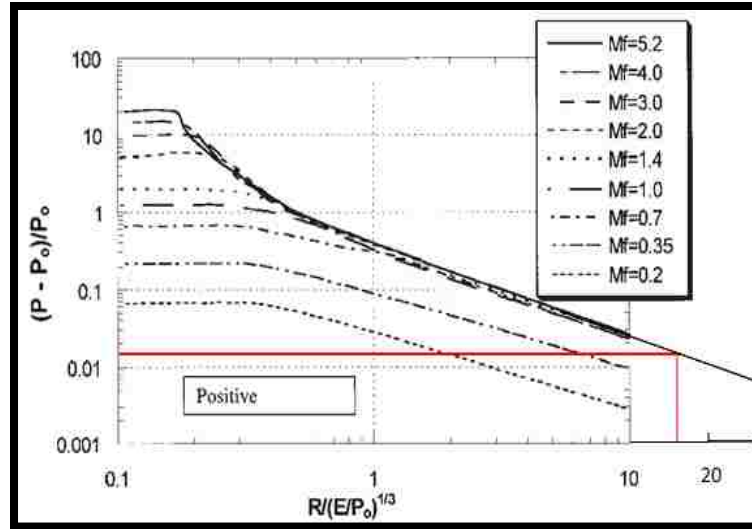


Figure 29 VCE characteristic by BST method (Pierorazio et al. 2005).

After estimating explosion energy, overpressure can be found at any location from cloud center. For instance, calculations for 20 ft are presented here. From equation 2, X-axis is about 1.6 which corresponds to dimensionless overpressure (Y-axis) of about 0.23. As a result, incident pressure will be equal to 3.38 psi and reflected pressure for zero angle of incident corresponds to 7.3 psi. Predicted overpressures for other locations around blast center are illustrated in Table 6. All calculations of overpressure prediction were developed in appendix A.

Table 6 Predicted pressure and incident's damage for various distances (BST method).

Damage	Distance from blasting center (ft)	Incident Pressure (psi)	Reflected Pressure* (psi)
Brick wall blown out	10	5.3	11.84
House demolished	20	3.38	7.3
Painting Shop (broken glass window)	93	0.5	0.79
Roller doors collapsed (front side)	120	0.38	0.76
Roller doors collapsed (back side)	155	0.3	0.3
Glass window breakage (ASTM E1300)	185	0.23	0.48
Bank slightly damaged and typical window breakage	450	0.09	0.18

*Reflected pressure coefficient calculations are explained in Appendix B.

7.4.2.2 Incident pressure (Pso) for both cases.

The different assumed flame speeds used in the BST method predictions could each potentially describe the actual pressure wave value that generated from Allentown's VCE explosion. Hence, an analysis was developed to compare the relation between the different flame speed (M_f 0.66, 0.7, and 0.93). Table 7 illustrates the incident pressures of both the assumed flame speeds for selected values of R. As a result, the analysis shows that both case studies resulted in similar values of overpressure when R beyond 14 feet; while a conspicuous change for values of overpressure appeared below 14 feet (Figure 30). In fact, width of the single house is about 15 ft. Thus, this might explain the

significant role of congestion level and degree of confinement inside the house to alter the value of overpressure.

Table 7 Incident pressure for both case studies

Incident pressure (Pso), psi			
R, ft	Flame speed (Mf)		
	0.66	0.7	0.93
BC	9.26	10.0	16.32
10	4.9	5.3	5.97
14	4.85		
20	3.38		

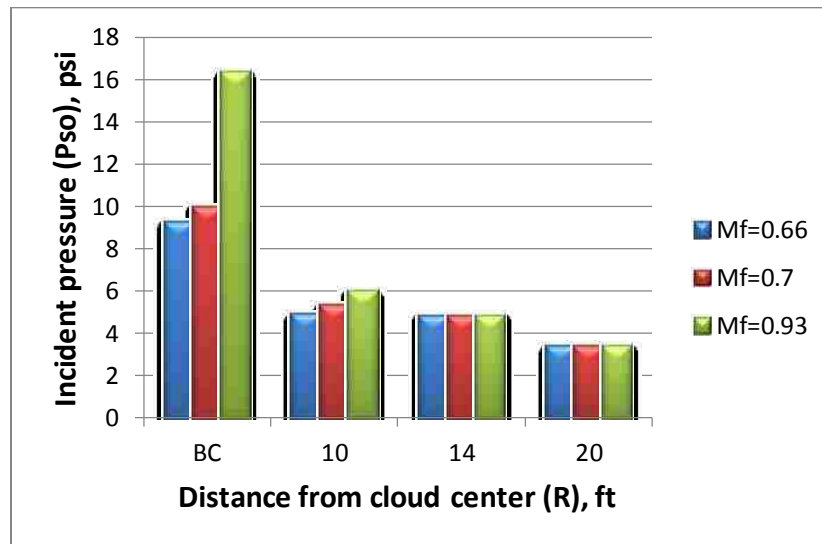


Figure 30 Incident pressure for both flame speeds.

7.4.3. Modified Bernoulli equation (MBE)

The MBE is a relationship between explosive velocity and pressure (equation 3). MBE has been commonly used to define pressure and velocity that resulted from explosion of a gas reservoir (Wilson, 1980). Projectile debris from the events is analyzed using the MBE to further verify the predicted overpressure values from the TNO and BST methods. Projectile velocity (V_0) at MBE can be found from equation 4.

$$\frac{1}{2} V_0^2 = \frac{P_i - P_o}{S} \quad (3)$$

$$V_0 = \sqrt{\frac{R \times g}{\sin 2\theta}} \quad (4)$$

Where V_0 is initial velocity; P_i is initial pressure; P_o is atmospheric pressure; S is density of an item; R is projectile distance; g is gravity acceleration; and θ is projectile angle.

Several photos of Allentown's NG explosion showed the resulting debris around the demolished houses. A piece of wood, located opposite to the exploded houses, was selected to be analyzed by the MBE (Figure 31). An assumption was provided for the projectile distance since there was no exact information about the piece of wood's initial location. Therefore, the assumption considered the piece of wood was ejected from blast center or 10 feet from blast center which corresponds to a distance of 117.5 and 127.5 feet to projectile final location (Figure 32). Also, the projectile angle is assumed to be 45° and gravity acceleration is 32 ft/s^2 ; the density of wood is 37.5 lb/ft^3 . By importing

the known data into equation 3 and equation 4, the resulting initial pressures for both assumed locations are 29.7 and 31.1 psi, respectively. Hence, these values of initial pressure (projectile pressure) are within the ranges of reflected pressure values which were developed by the BST and TNO methods (Table 8).

Table 8 Reflected pressure between BC to 10 ft.

R, ft	Reflected pressure range, psi	
	Minimum	Maximum
BC	17.45	48.96
10	11.03	25.0



Figure 31 Parts of wood flied from the exploded house [3].



Figure 32 Estimated distances of the flied wood's parts.

7.5. Associated damage and injuries for Allentown's incident

This part of paper illustrates the associated structural damages and injuries that resulted from Allentown's NG explosion. Moreover, the associated damages and injuries were compared with results from previous research (Pape et al. 2010).

7.5.1. Associated damage and injuries within 20 ft from cloud center

The region within 20 ft from blast center was selected to be analyzed. This region almost covers the entire area of the demolished houses. The range of the overpressure for both methods (the TNO and BST) for this region is illustrated in Table 9. Table 10 below shows the damages from various values of incident pressure (3.0 psi and higher) that were recorded from previous studies (Pape et al. 2010). An agreement was observed between the estimated damage in Table 10 and the actual damage that resulted in Allentown VCE where two houses were leveled, as mentioned before (Figure 33).

For this range of incident pressure, recorded injuries can vary from threshold for eardrum rupture to fatalities certain (Pape et al. 2010). As mentioned previously,

Allentown's explosion resulted in five fatalities of those living in the two demolished houses. Thus, the recorded injuries for developed incident pressures agreed with the real injuries in Allentown's accident

Table 9 Range of incident pressure within 20 ft

R, ft	Incident pressure range, psi	
	Minimum	Maximum
BC	7.35	16.32
20	3.23	3.68

Table 10 Type of damage when incident pressure more than 3.0 psi.†

Damage	Pressure (psi)	Reference
Roof cave in, block walls failed	3.0-5.0	Brasie and Simpson (1968)
Brick building severely damaged	5.0	Perry et al. (1997)
Brick walls broken	7.0-8.0	McIntyre et al. (1990)
Brick wall panel, 8 or 12 in. thick, not reinforced, shearing and flexural failures	7.0-8.0	Brasie and Simpson (1968), Crowl (2003) and FM Global Property (2008)
Roof blown off. Brick walls blown out. Steel frame largely intact and not distorted.	8.0-10.0	Brasie and Simpson (1968)
All conventional brick building destroyed	10.0	Perry et al. (1997)
Steel and brick building destroyed	≥ 10	Brasie and Simpson (1968)

† Information in the table has been collected from (Pape, Mniszewski, Longinow, & Kenner, 2010)



Figure 33 The demolished houses in Allentown's accident [6].

7.5.2. Associated damage between 30 to 185 ft

Beyond 30 ft from blast center, no severe damage was recorded in Allentown's NG explosion. However, a region between 30 to 185 feet from the cloud center was highlighted and analyzed where breakage of glass windows was the most observed damages (Figure 34; A, C and D). Incident pressure in this region ranges from 0.23 to 1.9 psi. Table 11 shows the damage that would result from this range of overpressure where shattering of glass windows is highly involved. Thus, a concurrence can be noticed between the damage in Allentown's incident and damage of the developed overpressure values by the BST and TNO methods.

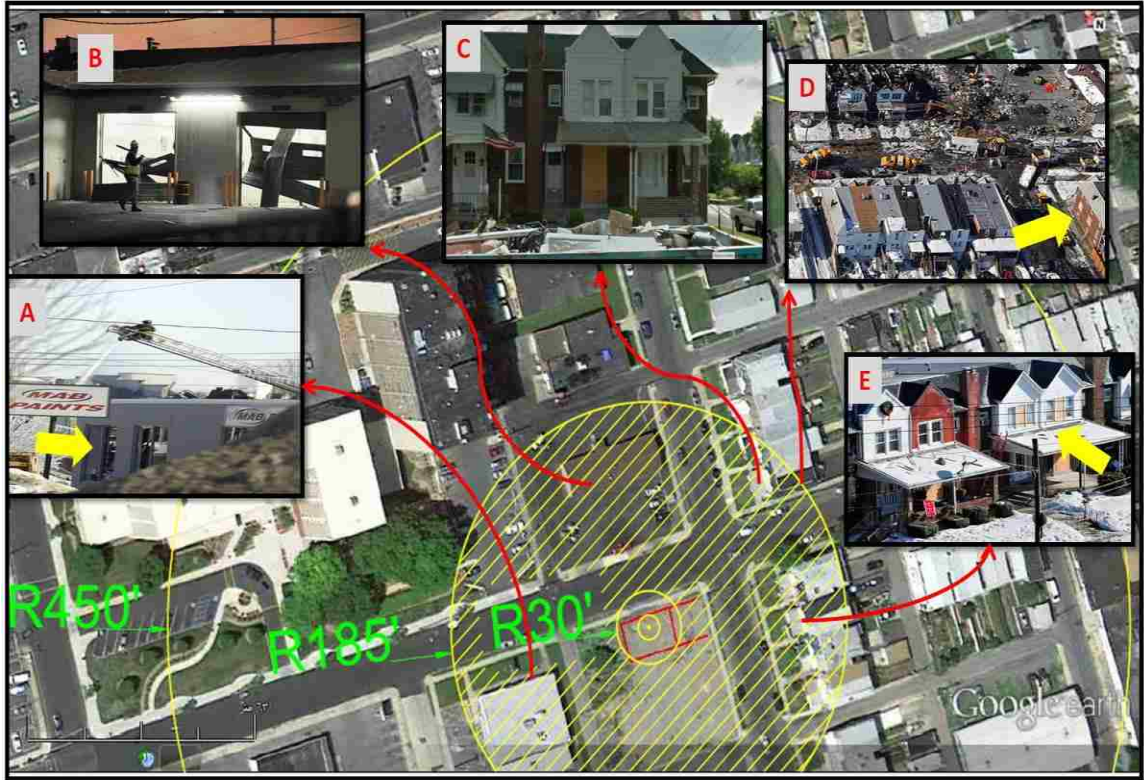


Figure 34 Locations and type of damage within 93 to 185 ft from blast center [7].

[6] <http://www.newsday.com/news/nation/cast-iron-gas-main-eyed-in-fatal-blast-1.2678488>

[7] (A, B) http://www.lehighvalleylive.com/allentown/index.ssf/2011/02/a_number_of_people_missing_af.html

(C) From Google map. (D&E) Morning call [3]

Table 11 Type of damage when incident pressure between 0.23 and 3.0 psi. †

Damage	Pressure (psi)	Reference
10 % window glass broken	0.29	CCPS (1994)
About 50% domestic glass broken	0.3	Perry <i>et al.</i> (1997)
Limit of minor structural damage	0.4 and 0.435	CCPS (1994), Stull. (1977), Crawl (2003), and NFPA (2008)
Shattering of glass window, large and small	0.5-1.0	Stull. (1977)
Window pane breakage (50% probability)	0.5-1.0	McIntyre <i>et al.</i> (1990)
Windows out. No structural damage	0.5-3.0	Brasie and Simpson (1968),

† Information in the table has been collected from (Pape, Mniszewski, Longinow, & Kenner, 2010)

7.5.3. Associated damage at 450 ft from cloud center

The NG explosion effectively reached a building located 450 feet from the blast center (Figure 35). The building is a two story steel frame structure with masonry exterior walls and curtain window walls; exterior walls consist of 8 inches Concrete Masonry Unit (CMU) and 4 inches veneer brick, according to Benesch (2011). In addition, since there is no x-bracing for the steel structure system, Benesch (2011) considered CMU as a resistance system for lateral load. The associated damage from the NG explosion was shattering of windows on the west elevation (Figure 36) and dropping of ceiling tiles on the first floor (Benesch, 2011).

As mentioned earlier, the developed incident pressure on the building is 0.09 psi. The reflected pressure on west side of the building (glass window wall side) is 0.18 psi

(Appendix B). From (ASTM E1300-12a, 2012) and since annealed glass type and short duration were assumed, however, NFL for this building's window with dimensions of (145 x 45 x 1/4) inches is about 0.13 psi (Figure 36). Consequently, breakage occurred because the applied reflected pressure was greater than the NFL for this window. In addition, occasional breaking for large window panes under strain was recorded at 0.03 psi, according to (CCPS, 1994). Thus, these verified as well the breakage of the window that occurred in the actual accident.

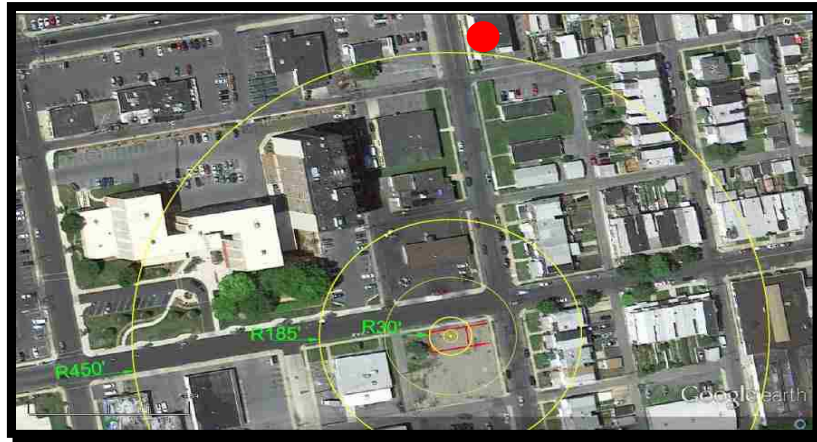


Figure 35 Location of the analyzed building at 450 ft from blast center.

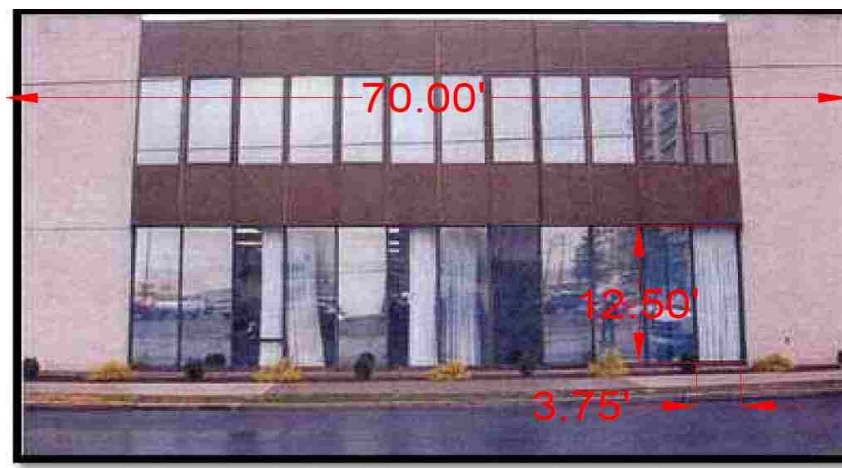


Figure 36 West elevation of the building (Benesch, 2011)

8. New York case study

On March 12, 2014, a two five stories brick buildings located in east Harlem in New York City collapsed from an explosion was caused by a NG leakage. Eight people died and more than seventy other were injured as a result of this accident (Siff & Russo, 2014). In addition, 100 households were evacuated from the neighborhood of the demolished buildings (Gregory, 2014). A report about NG leakage was received before the explosion and is officially considered as the main cause for the explosion (Siff & Russo, 2014). The pipelines that feed the two buildings were main cast-iron and plastic with low pressure and had a diameter of 12 inches. Currently, the pipelines have not been officially announced as the cause of the leakage (Siff & Russo, 2014).

Since the accident occurred 16 minutes after the report of the NG leakage (Erik et al. 2014), a partially CVCE was considered as the cause of Harlem's event. Similar to what was done earlier in this paper, locating the blast center is a significant step in predicting the VCE overpressure. Moreover, several glass windows were broken in this event. Thus, the appropriate glass window was selected to predict the overpressure of Harlem's VCE. These components will be presented more in depth this section.

8.1. Center of blast

Photos of the event indicate that the blast occurred inside the buildings where distribution of debris was all around the collapsed buildings (Figure 37). Figure 37- A&B shows debris from the explosion on a commuter railway (opposite to collapsed buildings) and on neighboring buildings. Furthermore, the powerful pressure from the VCE caused

the main structural system of the building to lose the ability to withstand its own weight (dead and live loads) which then resulted in a progressive collapsing of the buildings. Hence, the location of blast center is estimated in the middle of the two collapsed buildings (Figure 38).

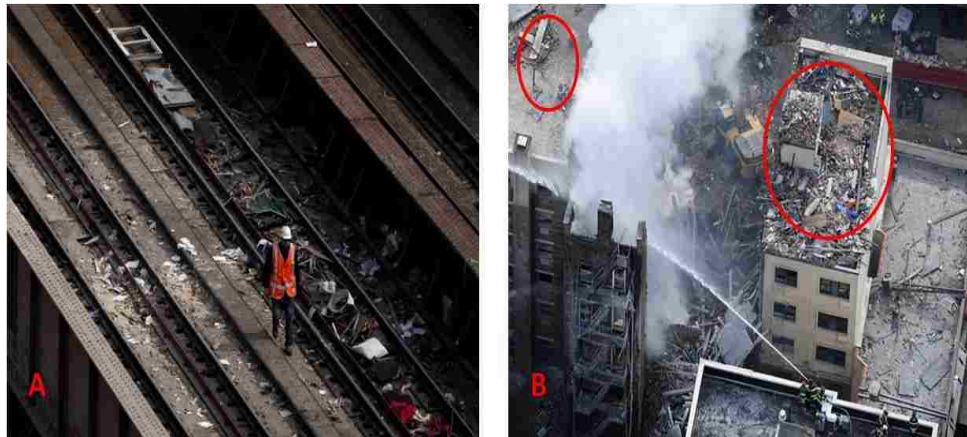


Figure 37 Debris distribution of NY's explosion [8].

8.2. Selection of the broken glass window

Several glass windows were broken in the incident. The window was selected based on the location and direction of the window. The selected glass window has the longest measured distance to the blast center of all the broken windows identified insuring the calculations using this location will provide the highest value of the explosion energy. Figure 38 shows the location of the selected glass window which is 155 feet from blast center. However, some of broken glass windows were also at the same distance as the selected window. Yet, the selected window is located indirectly from the normal blast waves ($\alpha > 90^\circ$) which results in a higher value when predicting

incident pressure than any other glass windows facing the blast waves (Figure 26). In other words, incident pressure on the selected window equals the reflected pressure.

The methodology to calculate the dimensions of the glass window in order to obtain incident pressure is similar to the one provided in Allentown case study. Thus, the dimensions of the selected glass window are estimated as 30 inches long, 27 inches width and 1/8 inches thickness (Figure 39). As mentioned before, (ASTM E1300-12a, 2012) developed charts to find NFL for domestic glass window. Again in this case study the type of the selected glass window is assumed to be annealed glass. In addition, short duration load was assumed for the selected windows. Thus, LR equals NFL. By importing the estimated dimensions into the selected chart, NFL corresponds to 0.47 psi (3.2 kPa) (Figure 40). In this particular case the value of reflected pressure is equivalent to incident pressure (P_{so}). Consequently, 0.47 psi is the reference value that will be utilized to predict overpressure at any other locations using the TNO and BST methods.



Figure 38 Blast center (BC) and selected glass window locations

[8] <http://www.nydailynews.com/new-york/uptown/death-toll-rises-7-east-harlem-explosion-article-1.1720134>



Figure 39 Dimensions of selected glass window.

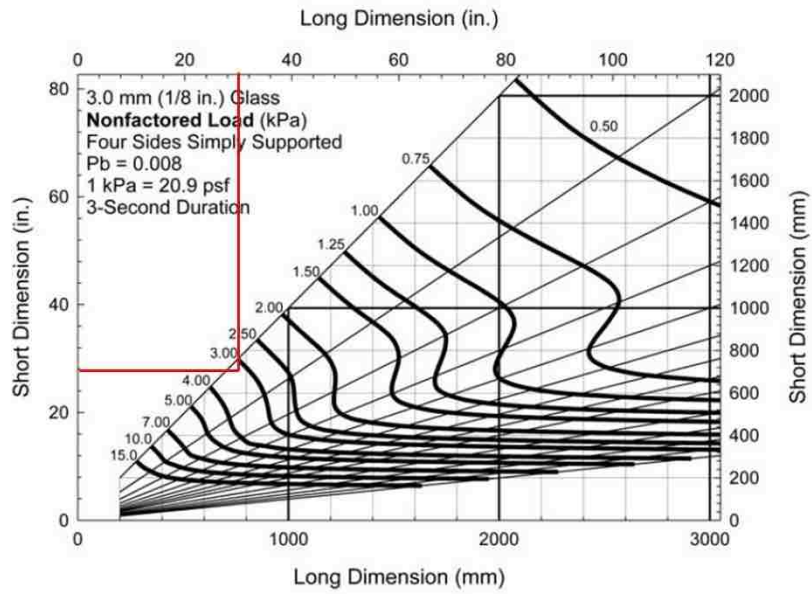


Figure 40 NFL for the selected glass window (ASTM E1300-12a, 2012).

8.3. Pressure prediction

The overpressure calculations for Harlem's case study use the same procedure as Allentown's case study. Therefore, only the explosion energy and predicted overpressure values at certain distances from blast center will be provided below.

8.3.1. TNO and BST method

For the TNO method, the explosion energy (E) that caused breakage for the selected glass window was calculated as 1.6E7 ft-lb. In addition, explosion energy (E) of the BST method corresponds to 1.54E7 ft-lb. As a result, predicted overpressure for the TNO and BST methods, for selected distances around blast center, is illustrated in Table 12 and Table 13, respectively. All calculations for both methods were presented in appendix C.

Table 12 Predicted pressure for various distances (TNO method).

Distance from blasting center (ft)	Incident Pressure (psi)	
	Curve no.	
	6	7
BC	7.35	14.7
10	7.35	13.52
30	3.23	3.68
40 (curves merge together)	2.35	
250	0.29	
450	0.14	

Table 13 Predicted pressure for various distances (BST method).

Distance from blasting center (ft)	Incident Pressure (psi)		
	Mf		
	0.66	0.7	0.93
BC	9.26	10.0	16.32
10	6.68	7.2	9.64
20 (curves merge together)	5.3		
30	3.23		
50	1.9		
250	0.29		
450	0.14		

8.4. Associated damages and injuries for New York's incident

The NG explosion energy and predicted overpressure of NY's incident indicate higher damages and injuries than Allentown's accident. Resulting damages from Harlem's NG explosion are presented in Figure 41 and Figure 42. The distribution of damages and injuries for selected distances were developed in this section.

8.4.1. Associated damages and injuries within 30 ft from cloud center

A radius of 30 feet around the center of Harlem's accident was highlighted to be analyzed. This region almost covered the area of the collapsed buildings. Therefore, a range for incident pressure was applied to consider minimum and maximum values for both methods (The TNO and The BST) within 30 ft (Table 14). The associated damage

for this range of incident pressure, which was recorded from former research (Pape et al. 2010), is presented in Table 10. As a result, the associated damages of the developed range agreed with the actual incident's damage where the two buildings were leveled within 30 feet (Figure 37-B).

The associated injuries for this range of incident pressure vary from threshold for eardrum rupture to fatalities certain (Pape et al. 2010). As mentioned earlier, Harlem's explosion recorded eight fatalities were found in the two demolished buildings.

Table 14 Range of incident pressure within 30 ft

R, ft	Incident pressure range, psi	
	Minimum	Maximum
BC	7.35	16.32
30	3.23	3.68

8.4.2. Associated damage between 30 to 250 ft

Most of the damage that was observed in this distance range was broken glass windows (Figure 41). For both methods (the TNO and the BST methods), incident pressure varied from 3.68 to 0.29 psi for the selected range. Previous research (Pape et al. 2010) indicates that broken glass windows are highly observed for this range of incident pressure (Table 11). Hence, a concurrence was observed for the damage of the predicated incident pressure and the actual damage at this radius in the Harlem event which is presented in Figure 41. Some of glass windows were examined individually by using (ASTM E1300-12a, 2012) in section 7.5.

8.4.3. Associated damage between 250 to 450 ft

Based on the available photos, little damage was noticed beyond 250 feet. The observed damage was mostly broken large glass windows, in this particular case typically those used in store fronts and church windows (Figure 42). Calculated incident pressure value, beyond 250 feet, is less than 0.29 psi. According to CCPS (1994), therefore, 10% of glass windows will be broken and occasional breaking of large windows panes under strain will occur when incident pressures are 0.29 and 0.03 psi, respectively. The predicted and real overpressure showed an agreement for the amount of damage in this region.



Figure 41 Associated damage between 30 to 250 ft [9]

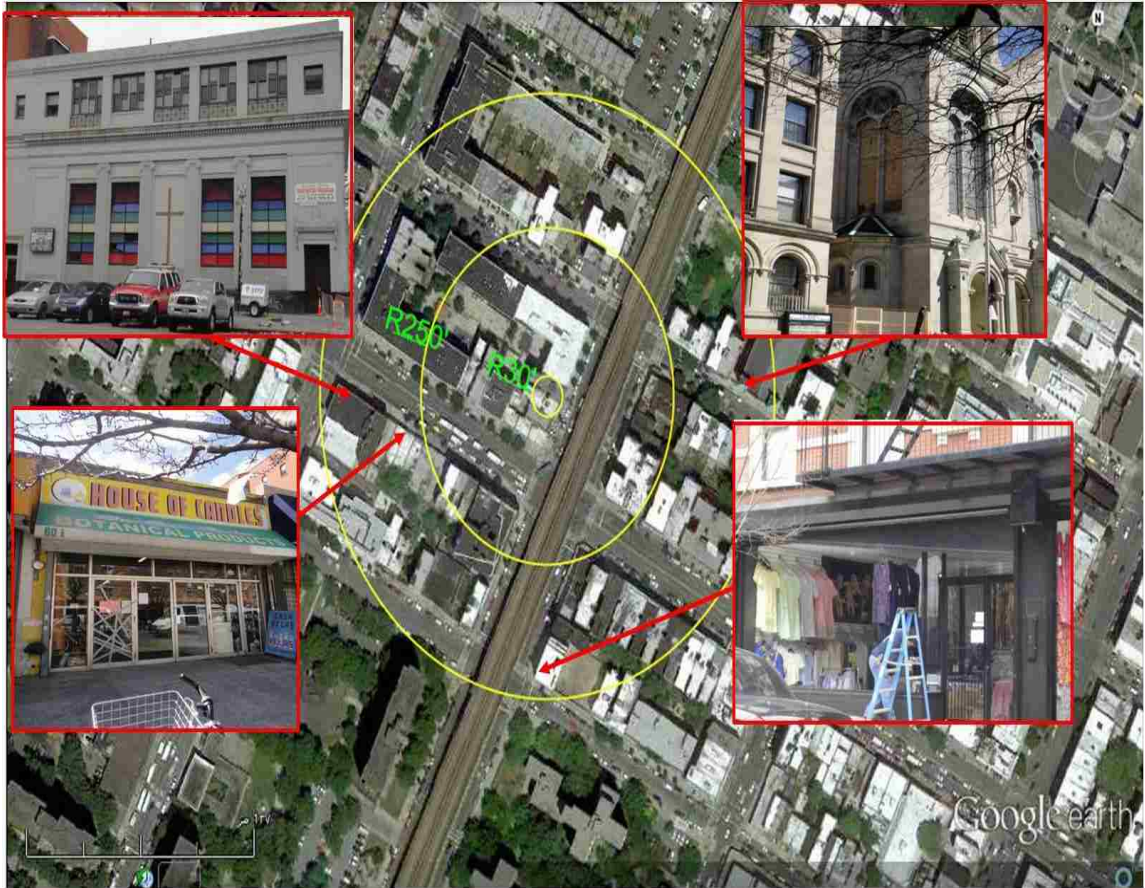


Figure 42 Associated damage between beyond 250 ft

[9] (A) <http://thenypost.files.wordpress.com/2014/03/collapse9.jpg>

(B) http://si.wsj.net/public/resources/images/BN-BW781_0312ha_H_20140312190601.jpg

8.5. Nonfactored and reflected load on glass window

The NG explosion caused the breakage of many glass windows in Harlem's accident. The reflected pressure, that caused breakage for glass windows, was compared with the NFL which is provided by (ASTM E1300-12a, 2012). The calculations for reflected pressure were explained before. Therefore, Table 15 shows the resulted values (Pro and NFL) of each selected glass window. All glass windows were assumed as annealed glass with a thickness of 1/8". In addition, short duration load was assumed for the selected windows. Figure 43 and Figure 44 illustrated locations and angle of the selected glass windows.

In the case of annealed glass and short duration load, breakage for glass window occurs when the applied uniform pressure exceeds the NFL. Table 15 shows that the NFL for both windows (A, B and C) is less than the applied reflected pressure (Pro). Thus, this verified the breakage for both glass windows in the real accident.

Table 15 Reflected and non-factored load for selected glass windows

Window no.	α , °	R, ft	Pso, psi	Pro, psi	NFL, psi
A	64	155	0.47	0.94	0.49
B	21	175	0.41	0.82	0.44
C	0*	185	0.38	0.76	0.28

*The shown angle (90°) for window no. C in Figure 43 is to verify that the window is facing the blast wave

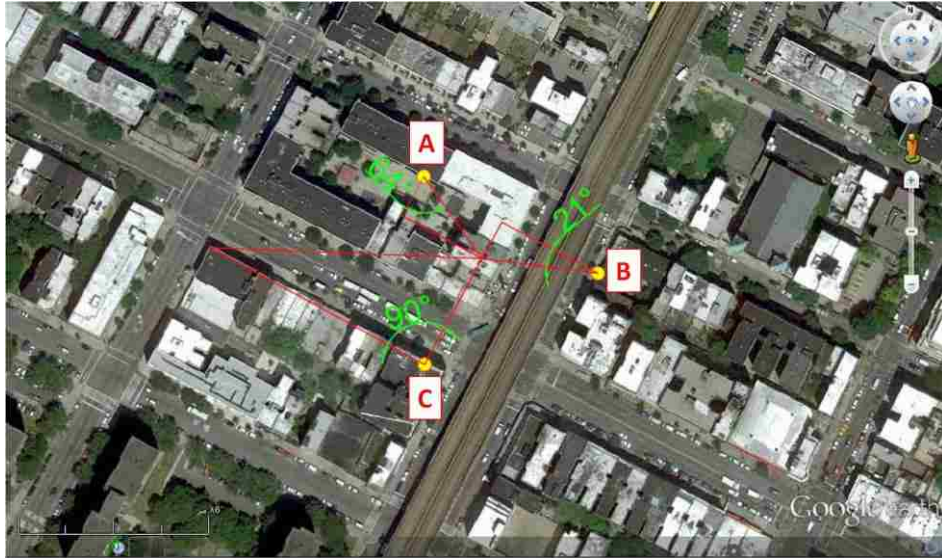


Figure 43 Locations and angle of selected glass windows



Figure 44 Selected glass windows. (A) [9]

8.6. Modified Bernoulli equation (MBE) (Harlem's accident)

In the Harlem accident, several pieces of debris were observed in front of a building that is located opposite to the demolished structures (Figure 45). A piece of wood was selected to be analyzed using MBE. The estimated projectile distances are 145 ft (from 10 ft from BC to final projectile location) and 155 ft (from BC to final projectile location) (Figure 45). As mentioned previously, in the Allentown case study, the projectile angle was assumed to be 45° and gravity acceleration is 32 ft/s^2 ; the density of wood is 37.5 lb/ft^3 . By importing the known data into equation 3 and equation 4, the initial pressures are equal to 33.5 and 34.7 psi. Hence, these values of projectile pressure are within the range of the reflected pressure values shown in Table 16.

Table 16 Reflected pressure between BC to 10 ft.

R, ft	Reflected pressure range, psi	
	Minimum	Maximum
BC	17.46	48.96
10	15.03	37.2

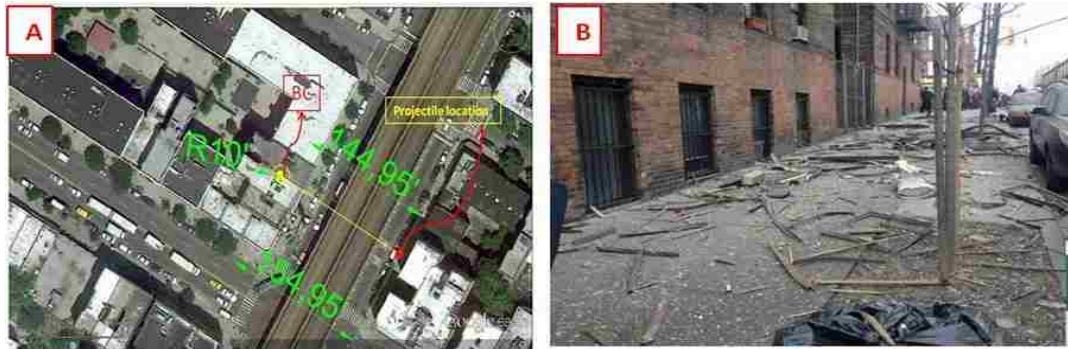


Figure 45 Location and distance of projectile debris [10]

{10} http://www.welcome2thebronx.com/wordpress/wp-content/uploads/2014/03/wpid-img_88756307823584.jpeg

9. Doubling explosion energy for both accidents (Allentown and Harlem)

In the case of an increased delay in ignition of these explosions, the vapor cloud volume would increase as well as explosion energy. The damage area, as a result, would grow and result in rising number of fatalities and injuries and cost of mending the associated damage. To better understand how the ignition time could have affected the explosion site the explosion energy (E) of Allentown's and New York's incident was doubled and analyzed using only the TNO method (curve number 7) to compare the damage of the potential scenario (doubling explosion energy) with the damage of the real incident. The analysis was developed by determining distance of the damage from the blast center for selected incident pressures. According to (Perry, et al., 1997), brick buildings will be severely damaged and nearly of 50% of domestic glass will be broken at incident pressures of 5.0 and 0.3 psi, respectively. Therefore, these two values of incident pressure (5.0 and 0.3 psi) were selected to compare the change in the area of damage of the assumed case to the real incident. Table 17 and Table 18 show the altered distances from blast center (R) to each selected incident pressure. This increase results in a 67% increase for Allentown and 64% increase for Harlem in severe damage to brick buildings and a 66% and 44% increase in the region over which window damage is likely to occur. The increase in area for both incident pressures is shown in Figure 46, Figure 47, Figure 48, and Figure 49. Based on the images it appears that the change in damage is not very sensitive to the amount of explosive where the radius of severe damage to brick buildings was not doubled but it only increased from 17 to 22 feet for Allentown and 25 to 32 feet

for Harlem accident. Calculations of overpressure for the assumed case are shown in appendix D.

Table 17 Distances of real and assumed explosion energy for selected Pso (Allentown)

Pso, psi	R, ft	
	Real	Assumed
5.0	17	22
0.3	155	200



Figure 46 Growing area of buildings damage for Allentown accident (Pso =5 psi)



Figure 47 Growing area of windows damage for Allentown accident (Pso=0.3 psi)

Table 18 Distances of real and assumed explosion energy for selected Pso

Pso, psi	R, ft	
	Real	Assumed
5.0	25	32
0.3	250	300



Figure 48 Growing area of buildings damage for Harlem accident (Pso =5.0 psi)

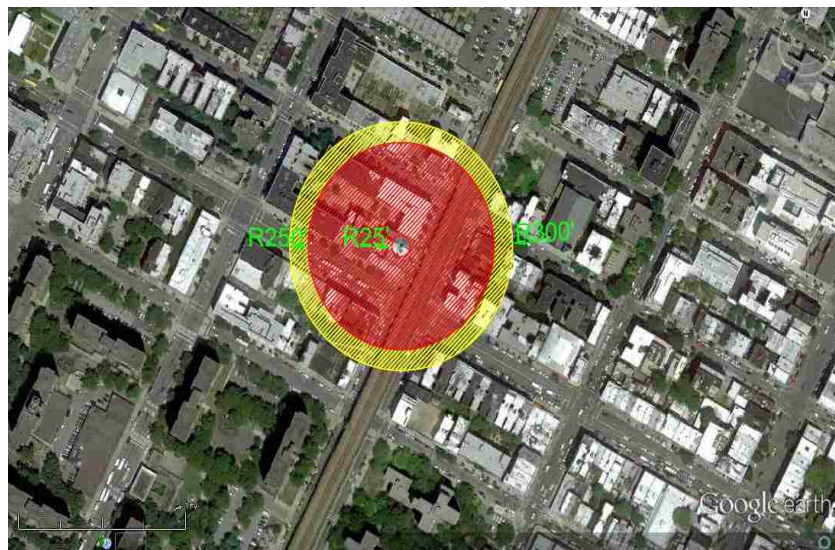


Figure 49 Growing area of windows damage for Harlem accident (Pso =0.3 psi)

10. Conclusion

In this paper, the BST and TNO methods were utilized to predict overpressure that was generated by accidental vapor cloud explosion in Allentown, PA and New York, NY. The explosion energy of the VCEs for the two case studies was calculated by using known window breakage strengths. The damage from the predicted overpressure correlated well with the actual damage observed in both Allentown and New York. Moreover, the load resistance of building glass windows provided by (ASTM E1300-12a, 2012) was compared with the incident pressure of the two explosions and verified the breakage that occurred for each glass windows in the actual accidents. In addition, MBE was used to calculate projectile pressure of debris that was thrown from explosion site, showing that MBE acquired values within the range for the BST and TNO results for both accidents (Allentown and Harlem). Finally, the growth in damage area in the case of delayed ignition of these two incidents (i.e. explosion energy was doubled) was compared with real incident damage area. Area of severe damage to brick building increased by 66% for Allentown and 64% for Harlem compared to the actual damage; while a 66% and 44% increase for region where window damage is likely to occur was seen. However, the change in damage is not very sensitive to the amount of explosive where the radius of severe damage to brick buildings was not doubled but it only increased from 17 to 22 feet for Allentown and 25 to 32 feet for Harlem accident.

11. References

- (CCPS), C. f. (1994). Guidelines for evaluating the characteristics of vapor cloud explosions, flash fires, and BLEVEs. *Center for Chemical Process Safety of the American Institute of Chemical Engineers.*
- ASME B31.8. (2003). Gas Transmission and Distribution Piping System. In T. U.S., *American Society of Mechanical Engineers.*
- ASTM E1300-12a. (2012). Standard Practice for Determining Load Resistance of Glass in Buildings. In *ASTM INTERNATIONAL.*
- Baker, M. J. (1999). A new set of blast curves from vapor cloud explosion . *Process Safety Progress.*
- Baker, Q. A., Tang, M. J., Scheler, E. A., & Sliva, G. J. (1999). Vapor Cloud Explosion Analysis. *Process Safety Progress, 15.*
- Benesch. (2011). *M&T Bank* . Allentown, PA.
- BERG, A. C. (1985). The Multi-energy Method. A framework for Vapor Cloud Explosion Blast Prediction. *Journal of Hazardous Materials, 12(1), 1-10.*
- Bjerketvedt, D., Bakke, J. R., & Wingerden, K. v. (1997). Gas Explosion Handbook. *Journal of Hazrdous Materials, 1-150.*
- Brasie, W. C., & Simpson, D. W. (1968). Guidelines for estimating damage explosion. *Journal of Loss Prevention in the Process Industries, 91-101.*

- Crowl, D. A. (1990). *Chemical process fundamentals with applications*. Englewood Cliffs, N.J: Prentice-Hall.
- Crowley, M. R. (2004). Evaluation of flammability hazards in non-nuclear safety. *14-th EFCOG Safety Analysis Workshop*. San Francisco, CA.
- DOD, D. o. (2008). Structures to Resist the Effects of Accidental Explosions. In *Unified Facilities Criteria UFC 3-340-02*. Washington, DC.
- Erik Badia, J. S. (2014, 03 14). Site of East Harlem explosion saturated with natural gas, suggesting leak caused blast: feds. New York, NY. Retrieved from <http://www.nydailynews.com/new-york/uptown/homeless-harlem-gas-blast-offered-housing-article-1.1721413>
- Gregory, K. (2014, 04 24). After blast, east Harlem tenant are worried about dust. New York, NY. Retrieved from http://www.nytimes.com/2014/04/25/nyregion/after-blast-east-harlem-tenants-are-worried-about-dust.html?_r=0
- Labor, U. D. (1990). *Phillips 66 Company Houston Chemical Explosion and Fire*.
- Lehman, P. (2011). *Coroner: Remains identified for Allentown explosion victim*. Retrieved from The Morning Call: http://articles.mcall.com/2011-02-15/news/mc-allentown-explosion-bea-hall-dna-20110215_1_gas-explosion-dna-testing-ugi-workers
- Lenoir, E. M. and Davenport, J. A. (1992). A Survey of Vapor Cloud Explosion-Second Update. *26th Loss Prevention Symposium*.

- M. J. Tang and Q. A. Baker. (1999). A New Set of Blast Curves from Vapor Cloud Explosion. *Process Safety Progress*, 18.
- Marx, T. A. (2008). *Estimating Flame Speeds for Use with the BST Blast Curves*. Norman, OK: Quest.
- McEvoy, C. (2012). *Allentown gas explosion caused by pipe recommended for replacement 30 years earlier*. Retrieved from Lehighvalleylive.com: http://www.lehighvalleylive.com/allentown/index.ssf/2012/06/pipe_that_caused_allentown_gas.html
- McEvoy, C. (2012, June 12). *Allentown gas explosion caused by pipe recommended for replacement 30 years earlier*. Retrieved from Lehigh Valley Live: http://www.lehighvalleylive.com/allentown/index.ssf/2012/06/pipe_that_caused_allentown_gas.html
- McIntyre, D. R. (1990). *Guidelines for assessing fire and explosion damage*. MTI Publication.
- Muhlbauer, W. K. (1996). *Pipeline risk management manual*. Houston: Gulf.
- NFPA. (2008). *Guide to fire and explosion investigation*. Quincy.
- Nolan, D. P. (2011). characteristic of hydrocarbon release, fires and explosions. In *Handbook of fire and explosion protection engineering principles: For oil, gas, chemical and related facilities*. Elsevier.
- Pape, R., Mniszewski, K. R., Longinow, A., & Kenner, M. (2010). *Explosion Phenomena and Effects of Explosions on Structures. III: Methods of Analysis (Explosion*

Damage to Structures) and Example Cases. *Practice Periodical on Structural Design and Construction*, 153-169.

Parfomak, P. W. (2013). Keeping America's Pipelines Safe and Secure: Key Issues for Congress. *Congressional Research Service*.

Perry, R., H., Green, D., W., Maloney, & J., O. (1997). *Perry's chemical engineer's handbook* (7th Ed. ed.). New York: McGraw-Hill.

PHMSA. (2014). *Significant Pipeline Incidents*. Retrieved from U.S. Department of Transportation: (1)

http://primis.phmsa.dot.gov/comm/reports/safety/sigpsi.html#_all (2)

<http://primis.phmsa.dot.gov/comm/NaturalGasPipelineSystems.htm?nocache=1832>

Pierorazio, A. J., Thomas, J. K., Baker, Q. A., & Ketchum, D. E. (2005). An Update to the Baker-Strehlow-Tang Vapor Cloud Explosion Prediction Methodology Flam Speed Table. *Process Safety Progress*.

Property, F. G. (2008). Guidelines for Evaluating the effects of vapor cloud explosions using a TNT equivalency method. *Loss prevention data sheets*.

Sheehan, D., Martinez, A., Assad, M., & Gamiz Jr., M. (2011). *Blast Kills Five & Coroner rules on cause of death for victims of Allentown explosion*. Retrieved from The Morning Call: http://articles.mcall.com/2011-02-10/news/mcallentown-gas-blast-fire-20110210_1_gas-explosion-reports-of-gas-odors-

apparent-gas-leak & http://articles.mcall.com/2011-02-11/news/mc-allentown-pa-gas-explosion-autopsi20110211_1_coroner-rules-explosion-fire-

Siff, A., & Russo, M. (2014, 03 14). *NYC Explosion Death Toll at 8, With 3 Still Missing in the Smoldering Rubble*. Retrieved from NBC New York: <http://www.nbcnewyork.com/news/local/Park-Avenue-116th-Street-Fire-Collapse-Explosion-249730131.html>

Stull, D. R. (1977). Fundamentals of fire and explosion, AIChE monograph series. *American Institute of Chemical Engineers, 73*.

Van den Berg, A. C. (1987). Blast Effects from Vapor Cloud Explosion. *International Conference on Vapor Cloud Modeling*. Cambridge, Massachusetts.

Wilson, L. (1980). Relationships between Pressure, Volatile Content and Eject Velocity in Three Types of Volcanic Explosion. *Journal of Volcanology and Geothermal Research, 297-313*.

Zeeuwen, J.P, and B.J. Wickema. (1978). The Measurement of Relative Reactivity of Combustible Gases. *Conference on Mechanisms of Explosions in Dispersed Energetic Materials*.

Appendix A: Overpressure prediction for Allentown's accident

A) Allentown's explosion overpressure prediction

When thickness of glass window equals to 1/8":

General knowns:

Atmospheric pressure: $P_o := 14.7 \text{ psi}$

Incident pressure at 185 ft (ASTM E1300): $P_{so} := 0.23 \text{ psi}$

Absolute pressure (P) $P := P_{so} + P_o = 14.93 \text{ psi}$

Distance from selected glass window to BC: $R_g := 185 \text{ ft}$

A-1) Prediction calculation by TNO method:

Y-axis corresponds to:

Dimensionless maximum side on overpressure: $\Delta P_s := \frac{P - P_o}{P_o} = 0.016$

From figure A-1, as a result, X-axis (R_r) corresponds to:

Combustion energy-scaled distance: $R_r := 14$

To obtain explosion energy (E):

$$\therefore R_r = R_g \cdot \left(\frac{P_o}{E}\right)^{\frac{1}{3}} \quad \text{or} \quad R_r = R_g \cdot \sqrt[3]{\frac{P_o}{E}}$$

$$\therefore \left(\frac{R_r}{R_g}\right)^3 = \left(\sqrt[3]{\frac{P_o}{E}}\right)^3$$

Explosion energy: $E := P_o \cdot \left(\frac{R_g}{R_r}\right)^3 = (4.884 \cdot 10^6) \text{ ft} \cdot \text{lb}$

The heat of combustion of an average stoichiometric hydrocarbon-air mixture: $e := 3.5 \cdot 10^6 \frac{\text{J}}{\text{m}^3} = (7.31 \cdot 10^4) \frac{\text{ft} \cdot \text{lb}}{\text{ft}^3}$

Vapor cloud volume: $V := \frac{E}{e} = 66.819 \text{ ft}^3$

After determining explosion energy, now Pso can be found at any locations from cloud center (Only curve number 7 has been explained below):

$$(1) \text{ Pso at 10 ft: } R_{10} := 10 \text{ ft}$$

$$\text{Combustion energy-scaled distance: } R_r := R_{10} \cdot \left(\frac{P_o}{E} \right)^{\frac{1}{3}} = 0.757$$

This value of X-axis in figure A-1 which corresponds to: $\Delta P_s := 0.68$

$$\therefore P_{so@10ft} := \Delta P_s \cdot P_o = 9.996 \text{ psi}$$

$$(2) \text{ Pso at 14 ft: } R_{14} := 14 \text{ ft} \quad (\text{Curves merge beyond this distance})$$

$$\text{Combustion energy-scaled distance: } R_r := R_{14} \cdot \left(\frac{P_o}{E} \right)^{\frac{1}{3}} = 1.059$$

This value of X-axis in figure A-1 which corresponds to: $\Delta P_s := 0.47$

$$\therefore P_{so@14ft} := \Delta P_s \cdot P_o = 6.909 \text{ psi}$$

$$(3) \text{ Pso at 17 ft: } R_{17} := 17 \text{ ft}$$

$$\text{Combustion energy-scaled distance: } R_r := R_{17} \cdot \left(\frac{P_o}{E} \right)^{\frac{1}{3}} = 1.286$$

This value of X-axis in figure A-1 which corresponds to: $\Delta P_s := 0.34$

$$\therefore P_{so@17ft} := \Delta P_s \cdot P_o = 4.998 \text{ psi}$$

Brick building severely damages within this distance (Perry, et al., 1997).

(4) Pso at 20 ft: $R_{20} := 20 \text{ ft}$

Combustion energy-scaled distance: $R_r := R_{20} \cdot \left(\frac{P_o}{E}\right)^{\frac{1}{3}} = 1.514$

This value of X-axis in figure A-1 which corresponds to: $\Delta P_s := 0.25$

$\therefore P_{so@20ft} := \Delta P_s \cdot P_o = 3.675 \text{ psi}$

(5) Pso at 93 ft: $R_{93} := 93 \text{ ft}$

Combustion energy-scaled distance: $R_r := R_{93} \cdot \left(\frac{P_o}{E}\right)^{\frac{1}{3}} = 7.038$

This value of X-axis in figure A-1 which corresponds to: $\Delta P_s := 0.034$

$\therefore P_{so@93ft} := \Delta P_s \cdot P_o = 0.5 \text{ psi}$

(6) Pso at 120 ft: $R_{120} := 120 \text{ ft}$

Combustion energy-scaled distance: $R_r := R_{120} \cdot \left(\frac{P_o}{E}\right)^{\frac{1}{3}} = 9.081$

This value of X-axis in figure A-1 which corresponds to: $\Delta P_s := 0.026$

$\therefore P_{so@120ft} := \Delta P_s \cdot P_o = 0.382 \text{ psi}$

(7) Pso at 155 ft: $R_{155} := 155 \text{ ft}$

Combustion energy-scaled distance: $R_r := R_{155} \cdot \left(\frac{P_o}{E}\right)^{\frac{1}{3}} = 11.73$

This value of X-axis in figure A-1 which corresponds to: $\Delta P_s := 0.02$

$\therefore P_{so@155ft} := \Delta P_s \cdot P_o = 0.294 \text{ psi}$

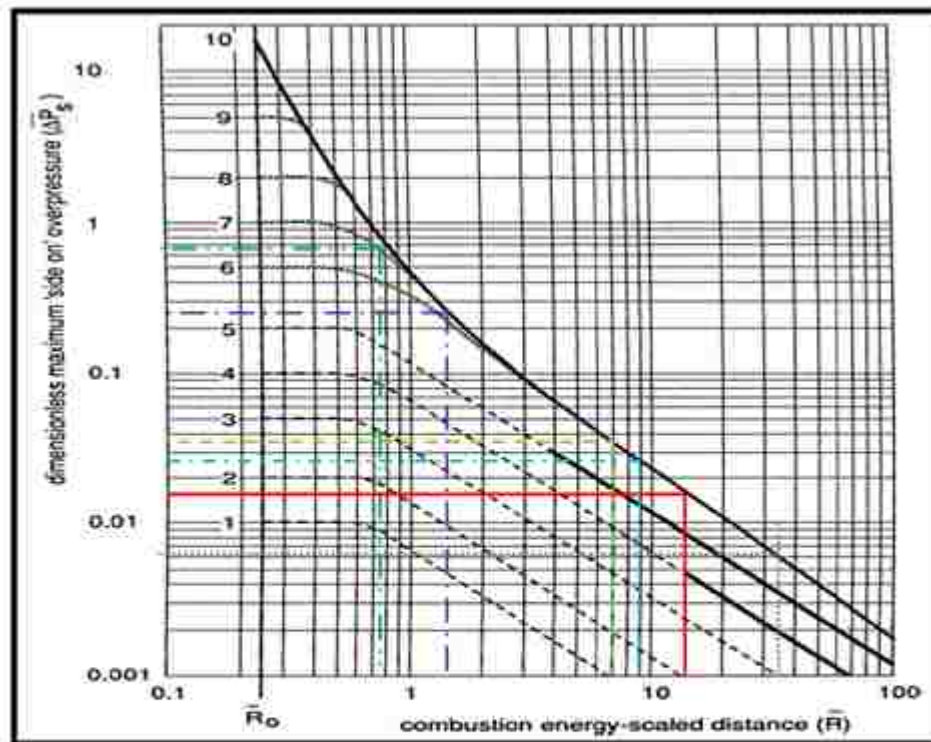
50% of domestic glass window broken within this distance (Perry, et al., 1997).

(8) Pso at 450 ft: $R_{450} := 450 \text{ ft}$

Combustion energy-scaled distance: $R_r := R_{450} \cdot \left(\frac{P_o}{E}\right)^{\frac{1}{3}} = 34.054$

This value of X-axis in figure A-1 which corresponds to: $\Delta P_s := 0.006$

$\therefore P_{so@450ft} := \Delta P_s \cdot P_o = 0.088 \text{ psi}$



	Distance from blast center		Distance from blast center
	10 ft		120 ft
	20 ft		185 ft
	93 ft		450 ft

Figure A-1

A-2) Prediction calculation by BST method :

Y-axis corresponds to:

$$\Delta P_s := \frac{P - P_o}{P_o} = 0.016$$

From figure A-2, as a result, X-axis (R_r) corresponds to:

Combustion energy-scaled distance: $R_r := 15$

To obtain explosion energy (E):

$$\begin{aligned} \therefore R_r &= R_g \cdot \left(\frac{P_o}{E} \right)^{\frac{1}{3}} & \text{or} & & R_r &= R_g \cdot \sqrt[3]{\frac{P_o}{E}} \\ \therefore \left(\frac{R_r}{R_g} \right)^3 &= \left(\sqrt[3]{\frac{P_o}{E}} \right)^3 \end{aligned}$$

Explosion energy:

$$E := P_o \cdot \left(\frac{R_g}{R_r} \right)^3 = (3.971 \cdot 10^6) \text{ ft} \cdot \text{lbf}$$

The heat of combustion of an average stoichiometric hydrocarbon-air mixture:

$$e := 3.5 \cdot 10^6 \frac{\text{J}}{\text{m}^3} = (7.31 \cdot 10^4) \frac{\text{ft} \cdot \text{lbf}}{\text{ft}^3}$$

Vapor cloud volume:

$$V := \frac{E}{e} = 54.326 \text{ ft}^3$$

After determining explosion energy, now we can find Pso at any locations from cloud center:

$$(1) \text{ (i) Pso at 10 ft (case } Mf=0.35\text{): } R_{10} := 10 \text{ ft}$$

$$\text{Combustion energy-scaled distance: } R_r := R_{10} \cdot \left(\frac{P_o}{E} \right)^{\frac{1}{3}} = 0.811$$

This value of X-axis in figure A-2 which corresponds to: $\Delta P_s := 0.11$

$$\therefore P1_{so@10ft} := \Delta P_s \cdot P_o = 1.617 \text{ psi}$$

$$(1) \text{ (ii) Pso at 10 ft (case } Mf=0.7\text{): } R_{10} := 10 \text{ ft}$$

$$\text{Combustion energy-scaled distance: } R_r := R_{10} \cdot \left(\frac{P_o}{E} \right)^{\frac{1}{3}} = 0.811$$

This value of X-axis in figure A-2 which corresponds to: $\Delta P_s := 0.36$

$$\therefore P2_{so@10ft} := \Delta P_s \cdot P_o = 5.292 \text{ psi}$$

$$(1) \text{ (iii) Pso at 10 ft (case } Mf=1.4\text{): } R_{10} := 10 \text{ ft}$$

$$R_r := R_{10} \cdot \left(\frac{P_o}{E} \right)^{\frac{1}{3}} = 0.811$$

This value of X-axis in figure A-2 which corresponds to: $\Delta P_s := 0.5$

$$\therefore P3_{so@10ft} := \Delta P_s \cdot P_o = 7.35 \text{ psi}$$

(1) (iii) Pso at 10 ft (for both cases Mf 0.93 and 0.66):

Since Mf 0.93 and 0.66 curves are not provided in BST chart, thus, an interpolation shall be applied to calculate Pso by using values of table A-2:

Table A-2 (Tang and Baker. 1999)

TABLE 1. M_s and M_w Relations		
M_w	M_s	P_{so}
0.057	0.07	0.010
0.074	0.12	0.028
0.125	0.19	0.070
0.250	0.35	0.218
0.500	0.70	0.680
0.750	1.00	1.240
1.000	1.40	2.000

$$\text{A) Case Mf 0.93: } P_{so@10ft} := P_{3so@10ft} - \left(\frac{1.4 - 0.93}{1.4 - 0.7} \cdot (P_{3so@10ft} - P_{2so@10ft}) \right) = 5.968 \text{ psi}$$

$$\text{B) Case Mf 0.66: } P_{so@10ft} := P_{2so@10ft} - \left(\frac{0.7 - 0.66}{0.7 - 0.35} \cdot (P_{2so@10ft} - P_{1so@10ft}) \right) = 4.872 \text{ psi}$$

(2) Pso at 14 ft: $R_{14} := 14 \text{ ft}$ (Curves merge beyond this distance)

$$\text{Combustion energy-scaled distance: } R_r := R_{14} \cdot \left(\frac{P_o}{E} \right)^{\frac{1}{3}} = 1.135$$

This value of X-axis in figure A-2 which corresponds to: $\Delta P_s := 0.33$

$$\therefore P_{so@14ft} := \Delta P_s \cdot P_o = 4.851 \text{ psi}$$

* Beyond 14 ft from blast center, Pso of different locations are equals for both cases since both cases' curves merge into one curve. Thus, calculations for both cases have been developed below

(3) Pso at 20 ft: $R_{20} := 20 \text{ ft}$

$$\text{Combustion energy-scaled distance: } R_r := R_{20} \cdot \left(\frac{P_o}{E} \right)^{\frac{1}{3}} = 1.622$$

This value of X-axis in figure A-2 which corresponds to: $\Delta P_s := 0.23$

$$\therefore P_{so@20ft} := \Delta P_s \cdot P_o = 3.381 \text{ psi}$$

(4) Pso at 93 ft: $R_{93} := 93 \text{ ft}$

$$\text{Combustion energy-scaled distance: } R_r := R_{93} \cdot \left(\frac{P_o}{E} \right)^{\frac{1}{3}} = 7.541$$

This value of X-axis in figure A-2 which corresponds to: $\Delta P_s := 0.034$

$$\therefore P_{so@93ft} := \Delta P_s \cdot P_o = 0.5 \text{ psi}$$

(5) Pso at 120 ft: $R_{120} := 120 \text{ ft}$

$$\text{Combustion energy-scaled distance: } R_r := R_{120} \cdot \left(\frac{P_o}{E} \right)^{\frac{1}{3}} = 9.73$$

This value of X-axis in figure A-2 which corresponds to: $\Delta P_s := 0.026$

$$\therefore P_{so@120ft} := \Delta P_s \cdot P_o = 0.382 \text{ psi}$$

(6) Pso at 450 ft: $R_{450} := 450 \text{ ft}$

$$\text{Combustion energy-scaled distance: } R_r := R_{450} \cdot \left(\frac{P_o}{E} \right)^{\frac{1}{3}} = 36.486$$

This value of X-axis in figure A-2 which corresponds to: $\Delta P_s := 0.006$

$$\therefore P_{so@450ft} := \Delta P_s \cdot P_o = 0.088 \text{ psi}$$

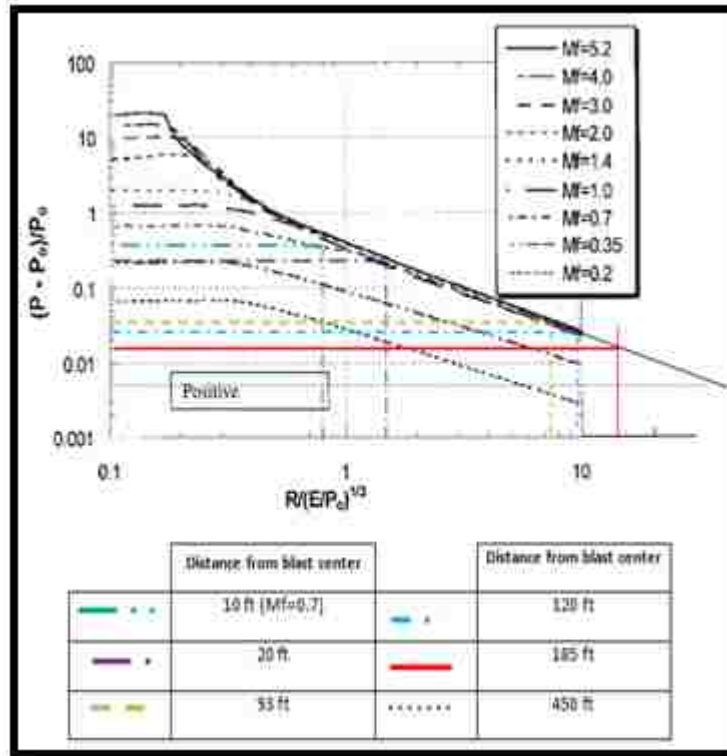


Figure A-2

Appendix B: Reflected pressure coefficient

In this part, reflected pressure coefficients for Allentown's accident have been developed below from Figure 26 (Tables B-(1 to 4)). Also, all angles of incident explained in figure B-1 below.

Table B-1: Reflected pressure coefficient for zero deg. angle of incident:

Cra	Pso (psi)	Pra (psi)	note
2	0.38	0.76	Roller door (front side)
2.168047	3.38	7.328	House demolished (BST method)
2.1739	3.68	8	House demolished (TNO method)
2.233962	5.3	11.84	Brick wall blown out (BST method)
2.5	10	25	Brick wall blown out (TNO method)

Table B-2: Reflected pressure coefficient for 84 deg. angle of incident:

Cra	Pso (psi)	Pra (psi)	note
1.5875	0.5	0.79375	Painting shop

Table B-3: Reflected pressure coefficient for 90 deg. angle of incident:

Cra	Pso (psi)	Pra (psi)	note
1	0.3	0.3	Roller door (backside)

Table B-4: Reflected pressure coefficient for 90 deg. angle of incident:

Cra	Pso (psi)	Pra (psi)	note
2	0.09	0.18	Glass window (bank)



Figure B-1 Angles of incident for various locations (Allentown accidents)

Appendix C: Incident pressure prediction for New York's accident

C) New York's explosion overpressure prediction

General knowns: when thickness for glass window 1/8 in

Atmospheric pressure: $P_o := 14.7 \text{ psi}$

Incident pressure at 155 ft (ASTM E1300): $P_{so} := 0.47 \text{ psi}$

Absolute pressure (P) $P := P_{so} + P_o = 15.17 \text{ psi}$

Distance from selected glass window to BC: $R_g := 155 \text{ ft}$

C-1) Prediction calculation by TNO method:

Y-axis corresponds to:

Dimensionless maximum side on overpressure: $\Delta P_s := \frac{P - P_o}{P_o} = 0.032$

From figure C-1, as a result, X-axis (R_r) corresponds to:

Combustion energy-scaled distance: $R_r := 7.9$

To obtain explosion energy (E):

$$\therefore R_r = R_g \cdot \left(\frac{P_o}{E}\right)^{\frac{1}{3}} \quad \text{or} \quad R_r = R_g \cdot \sqrt[3]{\frac{P_o}{E}}$$

$$\therefore \left(\frac{R_r}{R_g}\right)^3 = \left(\sqrt[3]{\frac{P_o}{E}}\right)^3$$

Explosion energy: $E := P_o \cdot \left(\frac{R_g}{R_r}\right)^3 = (1.599 \cdot 10^7) \text{ ft} \cdot \text{lb}_f$

The heat of combustion of an average stoichiometric hydrocarbon-air mixture: $e := 3.5 \cdot 10^6 \frac{\text{J}}{\text{m}^3} = (7.31 \cdot 10^4) \frac{\text{ft} \cdot \text{lb}_f}{\text{ft}^3}$

Vapor cloud volume: $V := \frac{E}{e} = 218.717 \text{ ft}^3$

After determining explosion energy, now we can find P_{so} at any locations from cloud center:

(1) P_{so} at 10 ft: $R_{10} := 10 \text{ ft}$

Combustion energy-scaled distance: $R_r := R_{10} \cdot \left(\frac{P_o}{E}\right)^{\frac{1}{3}} = 0.51$

This value of X-axis in figure C-1 when curve 6 selected: $\Delta P_s := 0.5$

$\therefore P_{so@10ft} := \Delta P_s \cdot P_o = 7.35 \text{ psi}$

This value of X-axis in figure C-1 when curve 7 selected: $\Delta P_s := 0.92$

$\therefore P_{so@10ft} := \Delta P_s \cdot P_o = 13.524 \text{ psi}$

(2) P_{so} at 20 ft: $R_{20} := 20 \text{ ft}$ (Curves equal or higher than no. 7 merge together beyond this point)

Combustion energy-scaled distance: $R_r := R_{20} \cdot \left(\frac{P_o}{E}\right)^{\frac{1}{3}} = 1.019$

This value of X-axis in figure C-1 which corresponds to: $\Delta P_s := 0.47$

$\therefore P_{so@20ft} := \Delta P_s \cdot P_o = 6.909 \text{ psi}$

(3) P_{so} at 25 ft: $R_{25} := 25 \text{ ft}$ (For curve number 7 only)

Combustion energy-scaled distance: $R_r := R_{25} \cdot \left(\frac{P_o}{E}\right)^{\frac{1}{3}} = 1.274$

This value of X-axis in figure C-1 which corresponds to: $\Delta P_s := 0.34$

$\therefore P_{so@25ft} := \Delta P_s \cdot P_o = 4.998 \text{ psi}$

Brick building severely damages within this distance (Perry, et al., 1997).

(4) Pso at 30 ft: $R_{30} := 30 \text{ ft}$ (For curve number 7 only)

$$\text{Combustion energy-scaled distance: } R_r := R_{30} \cdot \left(\frac{P_o}{E} \right)^{\frac{1}{3}} = 1.529$$

This value of X-axis in figure C-1 which corresponds to: $\Delta P_s := 0.25$

$$\therefore P_{so@30ft} := \Delta P_s \cdot P_o = 3.675 \text{ psi}$$

(5) Pso at 50 ft: $R_{50} := 50 \text{ ft}$

$$\text{Combustion energy-scaled distance: } R_r := R_{50} \cdot \left(\frac{P_o}{E} \right)^{\frac{1}{3}} = 2.548$$

This value of X-axis in figure C-1 which corresponds to: $\Delta P_s := 0.13$

$$\therefore P_{so@50ft} := \Delta P_s \cdot P_o = 1.911 \text{ psi}$$

(6) Pso at 185 ft: $R_{185} := 185 \text{ ft}$

$$\text{Combustion energy-scaled distance: } R_r := R_{185} \cdot \left(\frac{P_o}{E} \right)^{\frac{1}{3}} = 9.429$$

This value of X-axis in figure C-1 which corresponds to: $\Delta P_s := 0.026$

$$\therefore P_{so@185ft} := \Delta P_s \cdot P_o = 0.382 \text{ psi}$$

(7) Pso at 250 ft: $R_{250} := 250 \text{ ft}$

$$\text{Combustion energy-scaled distance: } R_r := R_{250} \cdot \left(\frac{P_o}{E} \right)^{\frac{1}{3}} = 12.742$$

This value of X-axis in figure C-1 which corresponds to: $\Delta P_s := 0.020$

$$\therefore P_{so@250ft} := \Delta P_s \cdot P_o = 0.294 \text{ psi}$$

50% of domestic glass window broken withing this distance (Perry, et al., 1997).

(5) Pso at 450 ft: $R_{450} := 450 \text{ ft}$

Combustion energy-scaled distance: $R_r := R_{450} \cdot \left(\frac{P_o}{E}\right)^{\frac{1}{3}} = 22.935$

This value of X-axis in figure C-1 which corresponds to: $\Delta P_s := 0.0095$

$\therefore P_{so@450ft} := \Delta P_s \cdot P_o = 0.14 \text{ psi}$

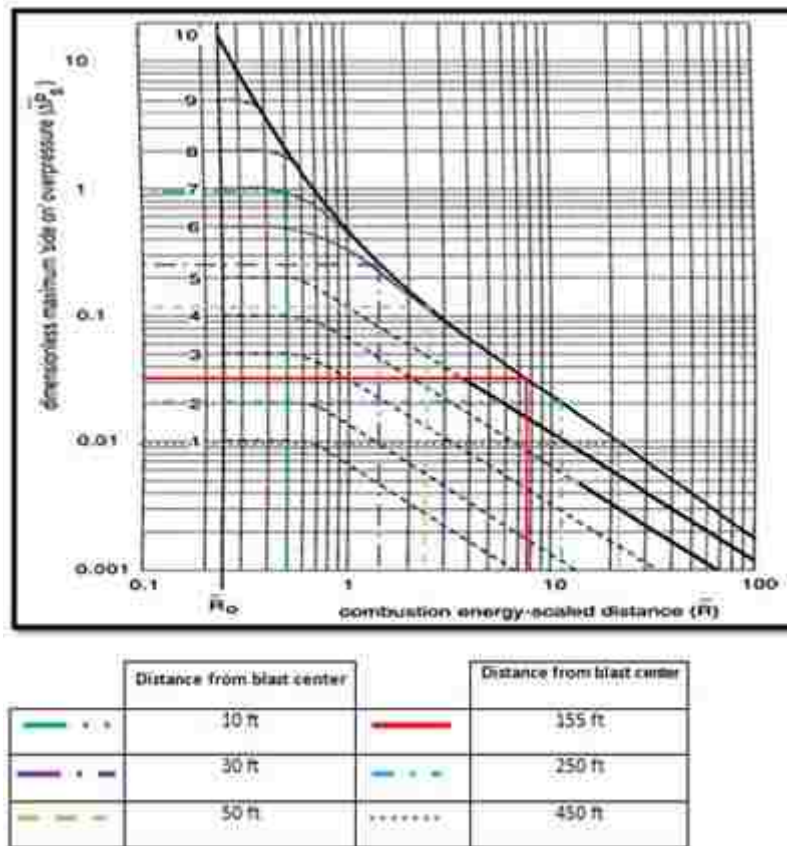


Figure C-1

C-2) Prediction calculation by BST method:

Y-axis corresponds to:

$$\Delta P_s := \frac{P - P_o}{P_o} = 0.032$$

From figure C-2, as a result, X-axis (R_r) corresponds to:

Combustion energy-scaled distance: $R_r := 8.0$

To obtain explosion energy (E):

$$\begin{aligned} \therefore R_r &= R_g \cdot \left(\frac{P_o}{E}\right)^{\frac{1}{3}} & \text{or} & & R_r &= R_g \cdot \sqrt[3]{\frac{P_o}{E}} \\ \therefore \left(\frac{R_r}{R_g}\right)^3 &= \left(\sqrt[3]{\frac{P_o}{E}}\right)^3 \end{aligned}$$

Explosion energy: $E := P_o \cdot \left(\frac{R_g}{R_r}\right)^3 = (1.54 \cdot 10^7) \text{ ft} \cdot \text{lb}_f$

The heat of combustion of an average stoichiometric hydrocarbon-air mixture: $e := 3.5 \cdot 10^6 \frac{\text{J}}{\text{m}^3} = (7.31 \cdot 10^4) \frac{\text{ft} \cdot \text{lb}_f}{\text{ft}^3}$

Vapor cloud volume: $V_2 := \frac{E}{e} = 210.617 \text{ ft}^3$

After determining explosion energy, now we can find P_{so} at any locations from cloud center:

$$(1) \text{ (i) Pso at 10 ft (Mf 0.35): } P1_{so@10ft} := 2.65 \text{ psi}$$

$$(1) \text{ (ii) Pso at 10 ft: } R_{10} := 10 \text{ ft}$$

$$\text{Combustion energy-scaled distance: } R_r := R_{10} \cdot \left(\frac{P_o}{E} \right)^{\frac{1}{3}} = 0.516$$

This value of X-axis in figure C-2 when Mf 0.7 selected: $\Delta P_s := 0.49$

$$\therefore P2_{so@10ft} := \Delta P_s \cdot P_o = 7.203 \text{ psi}$$

$$(1) \text{ (iii) Pso at 10 ft (Mf 1.4): } P3_{so@10ft} := 14.7 \text{ psi}$$

$$\text{A) Case Mf 0.93: } P_{so@10ft} := P3_{so@10ft} - \left(\frac{1.4 - 0.93}{1.4 - 0.7} \cdot (P3_{so@10ft} - P2_{so@10ft}) \right) = 9.666 \text{ psi}$$

$$\text{B) Case Mf 0.66: } P_{so@10ft} := P2_{so@10ft} - \left(\frac{0.7 - 0.66}{0.7 - 0.35} \cdot (P2_{so@10ft} - P1_{so@10ft}) \right) = 6.683 \text{ psi}$$

$$(2) \text{ Pso at 20 ft: } R_{20} := 20 \text{ ft} \quad \text{(In this distance, curves equal or higher than Mf 0.7 merge together)}$$

$$\text{Combustion energy-scaled distance: } R_r := R_{20} \cdot \left(\frac{P_o}{E} \right)^{\frac{1}{3}} = 1.032$$

This value of X-axis in figure C-2 which corresponds to: $\Delta P_s := 0.36$

$$\therefore P_{so@93ft} := \Delta P_s \cdot P_o = 5.292 \text{ psi}$$

$$(3) \text{ Pso at 25 ft: } R_{25} := 25 \text{ ft}$$

$$\text{Combustion energy-scaled distance: } R_r := R_{25} \cdot \left(\frac{P_o}{E} \right)^{\frac{1}{3}} = 1.29$$

This value of X-axis in figure C-2 which corresponds to: $\Delta P_s := 0.34$

$$\therefore P_{so@25ft} := \Delta P_s \cdot P_o = 4.998 \text{ psi}$$

Brick building severely damages within this distance (Perry, et al., 1997).

(4) Pso at 30 ft: $R_{30} := 30 \text{ ft}$

$$\text{Combustion energy-scaled distance: } R_r := R_{30} \cdot \left(\frac{P_o}{E} \right)^{\frac{1}{3}} = 1.548$$

This value of X-axis in figure C-2 which corresponds to: $\Delta P_s := 0.22$

$$\therefore P_{so@30ft} := \Delta P_s \cdot P_o = 3.234 \text{ psi}$$

(5) Pso at 50 ft: $R_{50} := 50 \text{ ft}$

$$\text{Combustion energy-scaled distance: } R_r := R_{50} \cdot \left(\frac{P_o}{E} \right)^{\frac{1}{3}} = 2.581$$

This value of X-axis in figure C-2 which corresponds to: $\Delta P_s := 0.13$

$$\therefore P_{so@50ft} := \Delta P_s \cdot P_o = 1.911 \text{ psi}$$

(6) Pso at 185 ft: $R_{185} := 185 \text{ ft}$

$$\text{Combustion energy-scaled distance: } R_r := R_{185} \cdot \left(\frac{P_o}{E} \right)^{\frac{1}{3}} = 9.548$$

This value of X-axis in figure C-2 which corresponds to: $\Delta P_s := 0.026$

$$\therefore P_{so@185ft} := \Delta P_s \cdot P_o = 0.382 \text{ psi}$$

(7) Pso at 250 ft: $R_{250} := 250 \text{ ft}$

$\frac{1}{3}$

$$\text{Combustion energy-scaled distance: } R_r := R_{250} \cdot \left(\frac{P_o}{E} \right)^{\frac{1}{3}} = 12.903$$

This value of X-axis in figure C-2 which corresponds to: $\Delta P_s := 0.020$

$$\therefore P_{so@250ft} := \Delta P_s \cdot P_o = 0.294 \text{ psi}$$

50% of domestic glass window broken within this distance (Perry, et al., 1997).

$$(8) P_{so} \text{ at } 450 \text{ ft: } R_{450} := 450 \text{ ft}$$

$$\text{Combustion energy-scaled distance: } R_r := R_{450} \cdot \left(\frac{P_o}{E} \right)^{\frac{1}{3}} = 23.226$$

This value of X-axis in figure C-2 which corresponds to: $\Delta P_s := 0.0095$

$$P_{so@450ft} := \Delta P_s \cdot P_o = 0.14 \text{ psi}$$

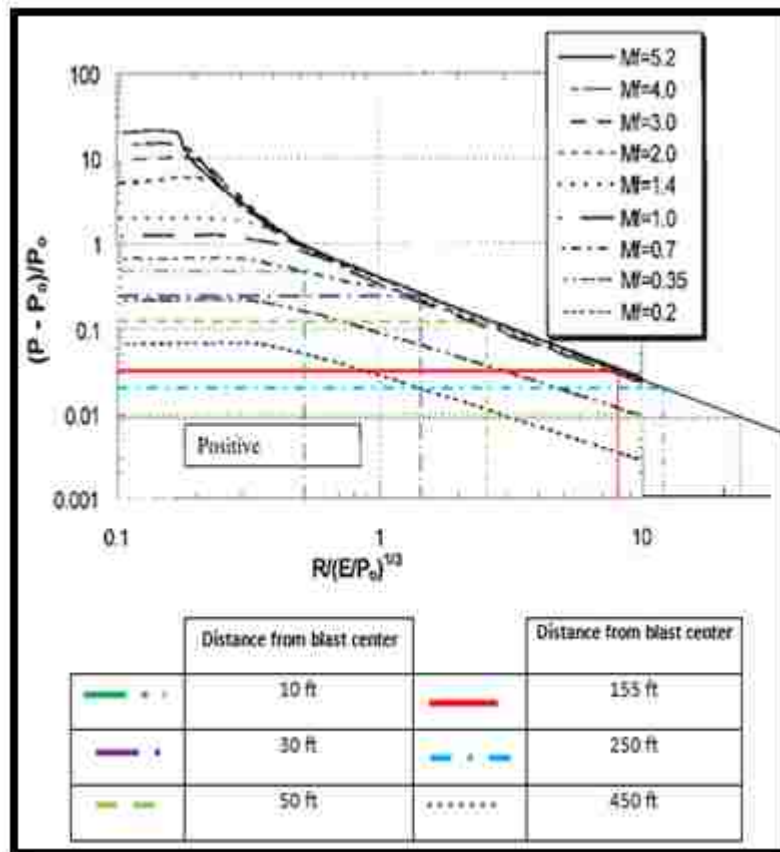


Figure C-2

Appendix D: Doubling explosion energy calculations for Allentown accident

D) Allentown's explosion overpressure prediction (Doubling explosion energy):

Atmospheric pressure: $P_o := 14.7 \text{ psi}$

Explosion energy (TNO method)
calculated before (appendix A): $E := 4884396.429 \text{ ft} \cdot \text{lb}$

Doubling explosion energy: $2 \cdot E = (9.769 \cdot 10^6) \text{ ft} \cdot \text{lb}$

After doubling explosion energy, now P_{so} can be determined at any locations from cloud center:

(1) P_{so} at 22 ft: $R_{22} := 22 \text{ ft}$

Combustion energy-scaled distance: $R_r := R_{22} \cdot \left(\frac{P_o}{2 \cdot E} \right)^{\frac{1}{3}} = 1.321$

This value of X-axis in figure D-1 which corresponds to: $\Delta P_s := 0.34$

$\therefore P_{so@32ft} := \Delta P_s \cdot P_o = 4.998 \text{ psi}$

Brick building severely damages within this distance (Perry, et al., 1997).

(2) P_{so} at 200 ft: $R_{200} := 200 \text{ ft}$

Combustion energy-scaled distance: $R_r := R_{200} \cdot \left(\frac{P_o}{2 \cdot E} \right)^{\frac{1}{3}} = 12.013$

This value of X-axis in figure D-1 which corresponds to: $\Delta P_s := 0.020$

$\therefore P_{so@300ft} := \Delta P_s \cdot P_o = 0.294 \text{ psi}$

50% of domestic glass window broken within this distance (Perry, et al., 1997).

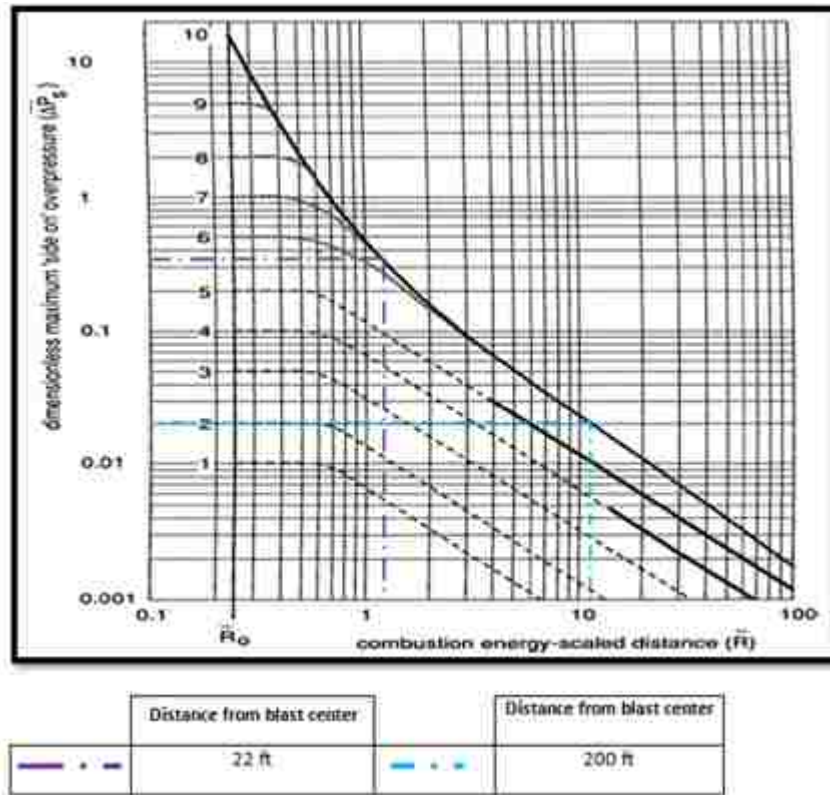


Figure D-1

Appendix E: Doubling explosion energy calculations for New York accident

E) New York's explosion overpressure prediction (Doubling explosion energy):

Atmospheric pressure: $P_o := 14.7 \text{ psi}$

Explosion energy (TNO method)
calculated before (appendix C): $E := 15987981.884 \text{ ft} \cdot \text{lb}$

Doubling explosion energy: $2 \cdot E = (3.198 \cdot 10^7) \text{ ft} \cdot \text{lb}$

After doubling explosion energy, now P_{so} can be determined at any locations from cloud center:

(1) P_{so} at 10 ft: $R_{10} := 10 \text{ ft}$

Combustion energy-scaled distance: $R_r := R_{10} \cdot \left(\frac{P_o}{2 \cdot E} \right)^{\frac{1}{3}} = 0.405$

This value of X-axis in figure D-1 when curve 7 selected: $\Delta P_s := 1.0$

$\therefore P_{so@10ft} := \Delta P_s \cdot P_o = 14.7 \text{ psi}$

(2) P_{so} at 25 ft: $R_{25} := 25 \text{ ft}$ (Curves equal or higher than no. 7 merge together beyond this point)

Combustion energy-scaled distance: $R_r := R_{25} \cdot \left(\frac{P_o}{2 \cdot E} \right)^{\frac{1}{3}} = 1.011$

This value of X-axis in figure D-1 which corresponds to: $\Delta P_s := 0.47$

$\therefore P_{so@25ft} := \Delta P_s \cdot P_o = 6.909 \text{ psi}$

(3) Pso at 32 ft: $R_{32} := 32 \text{ ft}$

$$\text{Combustion energy-scaled distance: } R_r := R_{32} \cdot \left(\frac{P_o}{2 \cdot E} \right)^{\frac{1}{3}} = 1.294$$

This value of X-axis in figure D-1 which corresponds to: $\Delta P_s := 0.34$

$$\therefore P_{so@32ft} := \Delta P_s \cdot P_o = 4.998 \text{ psi}$$

Brick building severely damages within this distance (Perry, et al., 1997).

(4) Pso at 155 ft: $R_{155} := 155 \text{ ft}$

$$\text{Combustion energy-scaled distance: } R_r := R_{155} \cdot \left(\frac{P_o}{2 \cdot E} \right)^{\frac{1}{3}} = 6.27$$

This value of X-axis in figure D-1 which corresponds to: $\Delta P_s := 0.040$

$$\therefore P_{so@155ft} := \Delta P_s \cdot P_o = 0.588 \text{ psi}$$

(5) Pso at 300 ft: $R_{300} := 300 \text{ ft}$

$$\text{Combustion energy-scaled distance: } R_r := R_{300} \cdot \left(\frac{P_o}{2 \cdot E} \right)^{\frac{1}{3}} = 12.136$$

This value of X-axis in figure D-1 which corresponds to: $\Delta P_s := 0.020$

$$\therefore P_{so@300ft} := \Delta P_s \cdot P_o = 0.294 \text{ psi}$$

50% of domestic glass window broken within this distance (Perry, et al., 1997).

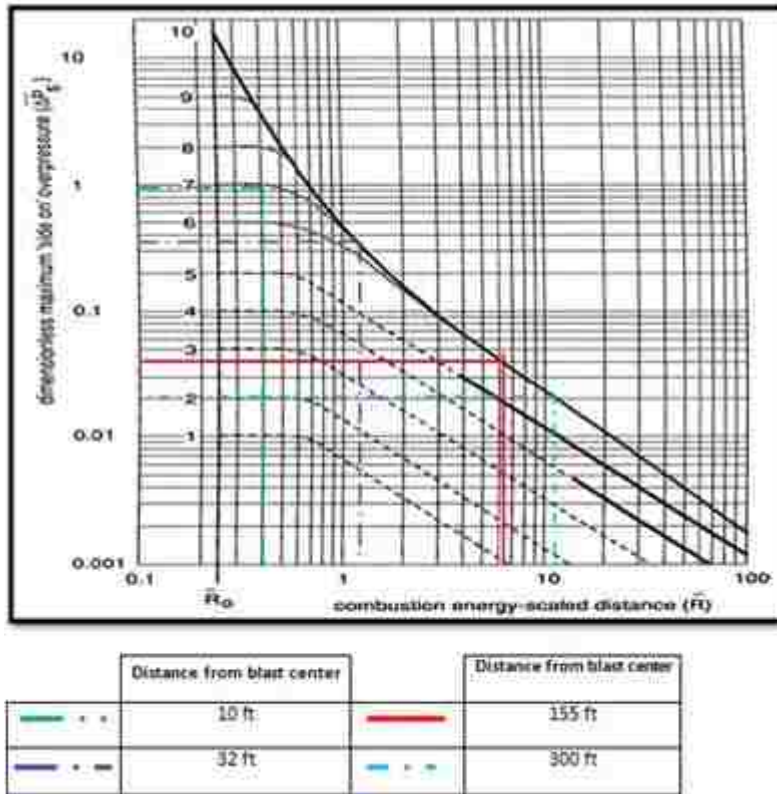


Figure E-1

Vita

Omar Mohammed Alawad, son of Mohammed Alawad and Hosah Almuseter, was born in March 10, 1987 in Buridah, Saudi Arabia. He earned his Bachelor degree in Civil Engineering in July 2010 from Qassim University. After graduation, Omar worked in a consultant office as a project engineer for three months. In January 2011, Omar received the approval to be one of the faculty members in Qassim University in Buridah, Saudi Arabia and to a scholarship to pursue his graduate study in the United States. In 2012, he accepted from Lehigh University to study Master of Science in Structural Engineering. He will receive his Master of Science in Structural Engineering in September 2014.